ELM control using external magnetic perturbations

Ilon Joseph
Fusion Energy Sciences Program, LLNL

13th International Workshop on Plasma Edge Theory
South Lake Tahoe
September 19th, 2011

This work performed under the auspices of the U.S. Department of Energy by Lawrence Livermore National Laboratory under Contract DE-AC52-07NA27344

LLNL-PRES-499531

Collaborators

Theory

• F. L. Waelbroeck	U. Texas-Austin
• R. Schneider, A. M. Runov	MPI Greifswald
• M. F. Heyn, I. B. Ivanov, S. V. Kasilov, W. Kernblicher	Univ. Graz
• C. S. Chang, G. Y. Park, H. R. Strauss	NYU-Courant
• V. I. Izzo	UCSD
• S. E. Kruger	Tech-X
• B. Dudson, S. Farley	Univ. York
• A. H. Boozer	Columbia Univ.
• M. S. Chance, J. K. Park	PPPL

Experiment

• T. E. Evans, T. H. Osborne, M. J. Schaffer	General Atomics
• M. E. Fenstermacher, M. Groth, C. J. Lasnier, M. J. Lanctot	LLNL
• H. Frerichs, M. Jakubowski, O. Schmitz	FZ-Julich
• J. A. Boedo, R. A. Moyer	UCSD
• G. R. Mckee	U. Wisconsin
• J. R. Watkins	Sandia National Lab

OUTLINE

- **Motivation**
- **Plasma Response to Applied Fields**
- **Transport Mechanisms**
- **Small-Island Transport**
- **Conclusions**

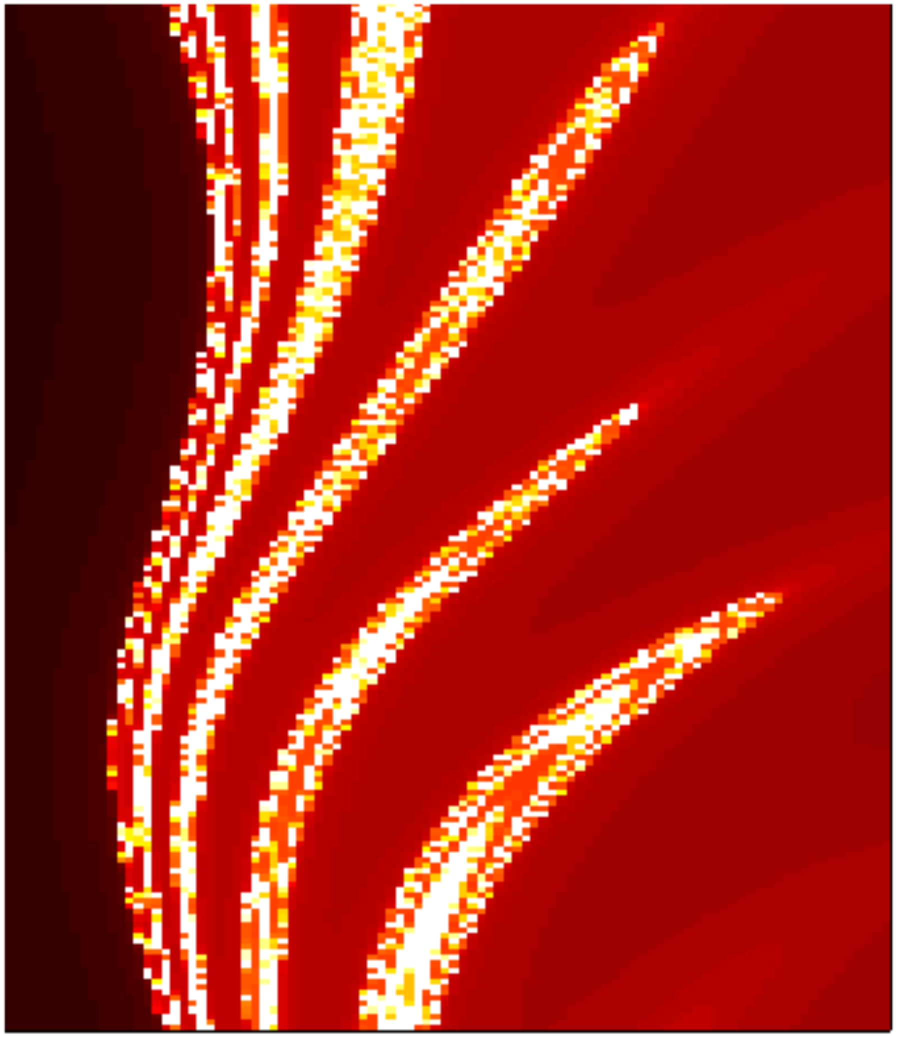

Understanding the physics of ELM control is a high priority!

- **ELM control is necessary for future tokamak-based fusion reactors**
  - Already a serious design consideration for ITER
  - And placing coils inside the vacuum vessel is very expensive!
  - In order to predict whether this method will scale to future devices, we need to understand both the ***enhanced transport*** and the ***requirements for control***

- **For each flavor of ELM control via external magnetic perturbations …**

– **ELM triggering:** Type-I ELM transport
  - Must be rapid enough to produce tolerable transport
  - ELM-free equilibrium transport determines the desired ELM frequency

– **ELM mitigation:** small ELM transport (not type-I?)
  - How does the RMP change the stability of small ELMs?
  - Or how does the RMP change the nonlinear evolution of type-I ELMs?

– **ELM suppression: transport mechanism unknown?**
  - Same mechanism responsible for increased T_e during ELM triggering?

What is the transport mechanism during ELM suppression?

- **Original idea: magnetic perturbations induce stochastic magnetic field**
  - But stochastic fields typically induce large electron thermal transport, not convective transport
  - Calculations suggest this is not likely without serious modification of either the perturbations inside the plasma or of electron thermal transport

- A more critical evaluation of the way that the magnetic perturbations penetrate into the plasma suggest that there is ***little actual reconnection***
  - Plasma must flow within magnetic surfaces
  - Perpendicular plasma flow must vanish if islands or stochastic fields are present
  - Large inertial/viscous forces drive a large shielding current

- **So what can be responsible for convective transport?**
  - 3D fields drive additional viscous transport
  - Experimentally, turbulence has also been shown to increase rapidly
  - Can we understand this from first principles?

OUTLINE

- Motivation
- **Plasma Response to Applied Fields**
  - Ideal MHD, shielding & RFA
  - Non-ideal reconnection physics
- Transport Mechanisms
- Small-Island Transport
- Conclusions

Plasma responds to an external magnetic perturbation both through amplification and shielding of perturbed flux

- Normal modes of ideal MHD are amplified

$$S_{ext} = \Psi_{ext} / \Psi_{vac} > 1$$

- Ideal MHD screens resonant fields near rational surface $m = qn$

$$\psi(x) = \psi_{int} \Psi_{tear}(x) + \psi_{ext} \Psi_{ideal}(x)$$

$$S_{int} = \Psi_{int} / \Psi_{ext} << 1$$

- Non-ideal physics near rational surface determines amount of reconnection
  - Plasma rotation provides screening

$$S_{rec} = \Psi_{rec} / \Psi_{int} \leq 1$$

- Total reconnected flux ~$S_L^{-1/3}$

$$T_{rec} = S_{rec} S_{int} S_{ext} << 1$$

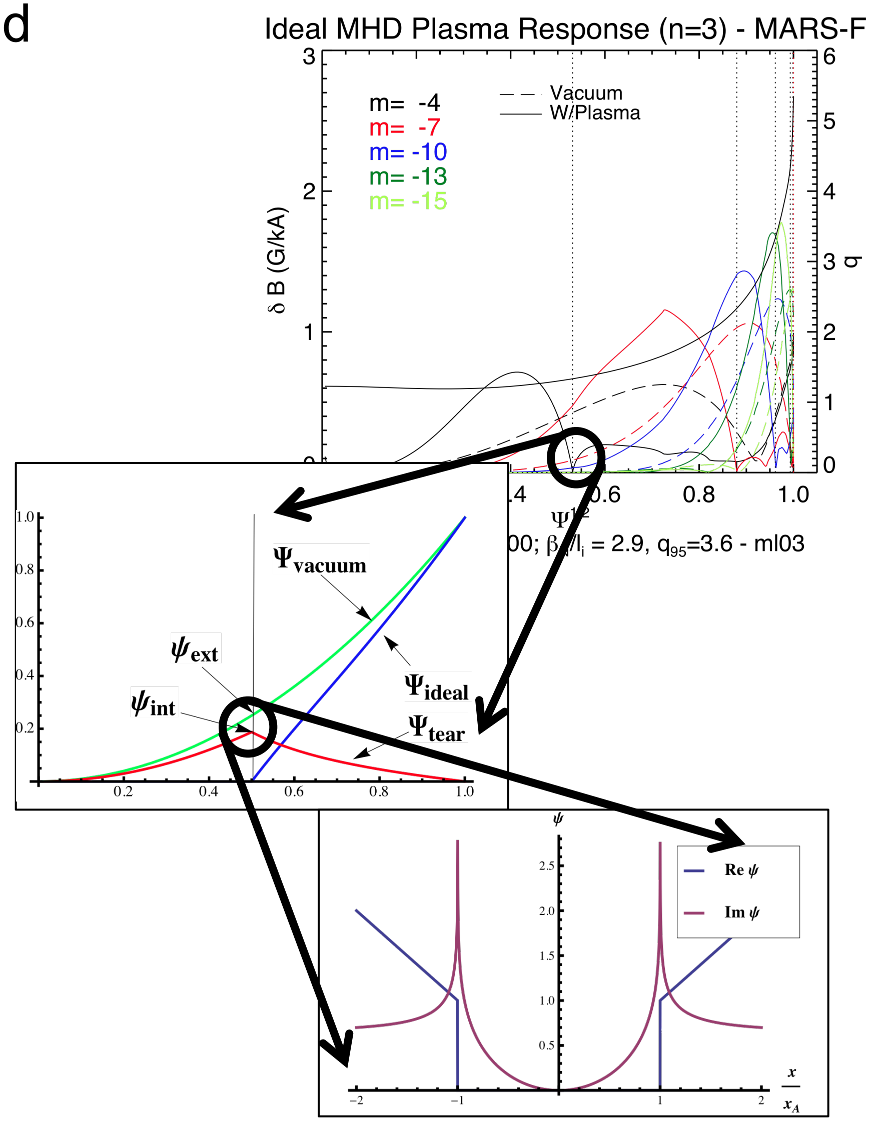

Ideal MHD holds far from resonant surfaces $k_{\|} = (m\text{-}nq)/qR \sim 0$

- The form of the exterior solution is dictated by ideal MHD
  - Decompose the perturbed flux ψ into an ideal shear Alfven wave Ψ_{ideal} and a tearing-parity mode Ψ_{tear}

$$\psi(x) = \psi_{int}\Psi_{tear}(x) + \psi_{ext}\Psi_{ideal}(x)$$

$$\Psi_{tear}(r_s) = 1 \qquad \Psi_{ideal}(r_s) = 0$$

$$\Psi_{tear}(a) = 0 \qquad \Psi_{ideal}(a) = (a/r_s)^m$$

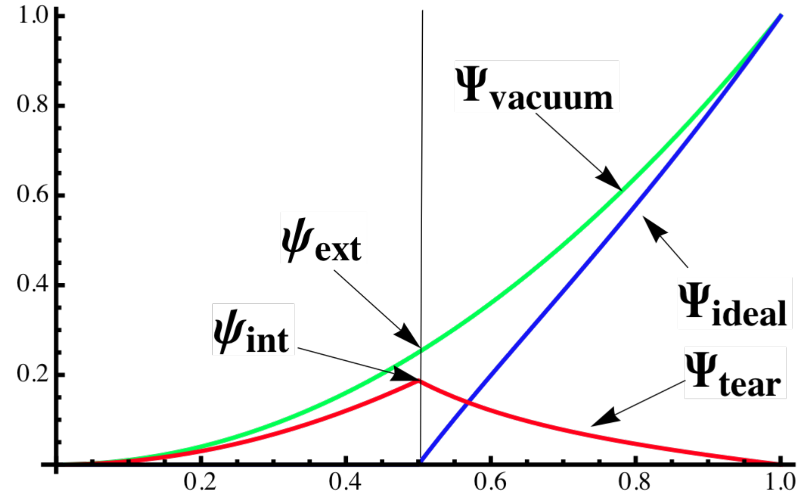

- Non-ideal effects near the rational surface determine the plasma impedance
  - The parallel current must be matched to the jump in the exterior solution

$$\Delta_{layer} = \left.\frac{\partial_x \psi}{\psi}\right|_{s-}^{s+} = -\frac{4\pi}{c}\frac{\int J_{\|}dx}{\psi_s} = \Delta'_{tear} + \Delta'_{ideal}\frac{\psi_{ext}}{\psi_{int}}$$

- **Transmission factor is the final output**
  - Conductivity effectively increases with rotation and shields reconnected flux

$$S_{int} = \frac{\psi_{int}}{\psi_{ext}} = \frac{-\Delta'_{ideal}/\Delta'_{tear}}{1-\Delta_{layer}/\Delta'_{tear}} \sim \frac{1}{\omega^{\alpha} S_L^{\beta}}$$

Fusion Energy Sciences

Reconnected flux ψ_{rec} is not equivalent to "internal flux" ψ_{int}

Example: Ideal MHD-Inertial regime[1]

- **2-field reduced MHD model**

$$\frac{d}{dt} = \frac{\partial}{\partial t} + \frac{\mathbf{b}\times\nabla\phi}{B}\cdot\nabla \qquad \frac{\partial\psi}{\partial t} = \nabla_{\parallel}\phi$$

$$U = \nabla_{\perp}^{2}\phi \qquad \frac{dU}{dt} = V_A^2\nabla\cdot J_{\parallel}$$

$$J_{\parallel} = \nabla_{\perp}^{2}\psi$$

  - **Dispersion assuming thin island limit**

$$\partial_x\left(\omega^2 - \left(k_{\parallel}V_A\right)^2\right)\partial_x\phi = 0 \qquad \partial_x >> \partial_y$$

- **Solution including magnetic shear**
  - **Has shear Alfven resonances at x_A**

$$k_{\parallel} = k_{\parallel}'x = k_y x/L_s \qquad \psi = x\phi/x_A$$

$$x_A = L_s\omega/k_y c \qquad \phi = i\left(2x_A/\pi\right)\arctan\left(x/x_A\right)$$

  - **Finite transmission but no reconnection!**

$$\Delta/2k_y = i\pi/k_y x_A = i\pi\omega_A/\omega$$

$$S_{int} = 1/(1 - i\omega_A/\pi\omega)$$

$$\boxed{\begin{aligned}\psi_{rec} &= \psi(x=0) = 0\\ S_{rec} &= \psi_{rec}/\psi_{int} = 0\end{aligned}}$$

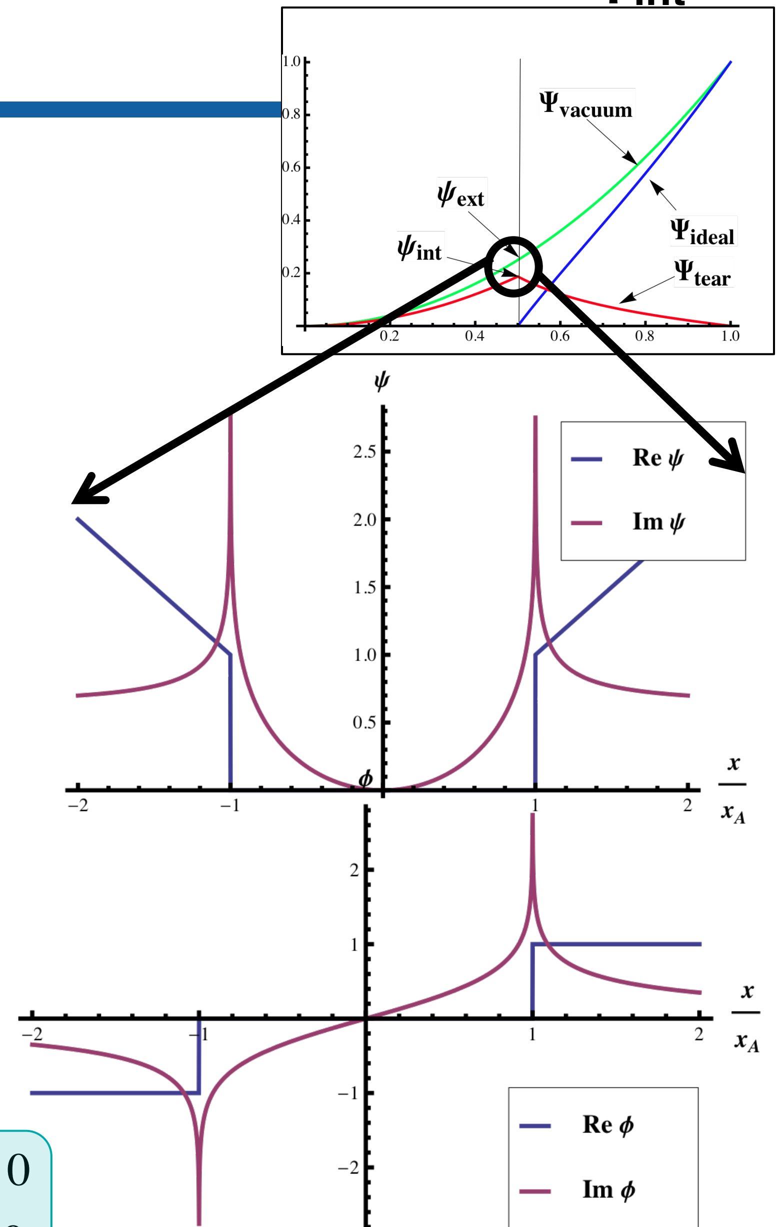

[1] A.H. Boozer, Phys. Plasmas **3** (1996) 4620

The exterior MHD solution is greatly affected by realistic plasma geometry and stability[1]

IPEC calculation by J. K. Park

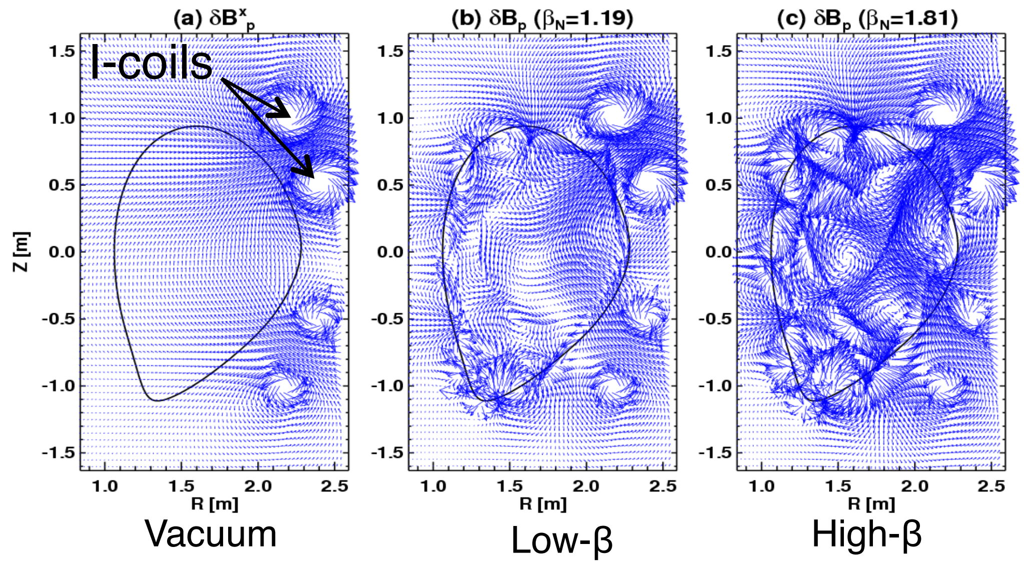

- **The plasma displacement $\xi(x)$ is a sum over normal modes**

$$\ddot{\xi}_n = F_{MHD}\xi_n = -\omega_n^2\xi$$

  - Response to an external source

$$\ddot{\xi} - F_{MHD}\xi = H(x)$$

$$\xi(x) = \sum_n \frac{\langle \xi_n^* H\rangle \xi_n(x)}{\omega_n^2 - \omega^2} \approx \sum_n \frac{\langle \xi_n^* H\rangle \xi_n(x)}{\omega_n^2}$$

  - Internal field is rather different from applied "vacuum" field!

- **Strong amplification near marginal stability[1]**
  - The least stable mode $\omega_0 = \min(|\omega_n|) \sim 0$ dominates

$$\boxed{\xi(x) \approx \frac{\langle \xi_0^* H\rangle \xi_0(x)}{\omega_0^2} \propto \frac{\langle \xi_0^* H\rangle \xi_0(x)}{1 - \beta/\beta_{crit}}}$$

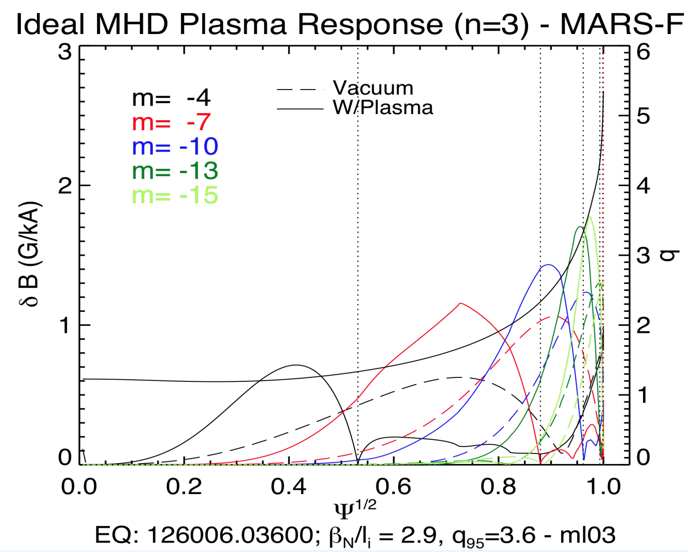

MARS-F calculation by M. J. Lanctot

[1] *A.H. Boozer, Phys. Plasmas* ***86*** *(2001) 5059*

RFA has important implications for ELM control: The spectrum must fit the plasma!

- Properly sculpted interaction can increase the perturbation strength of desired helicities locally; e.g. near the edge
  - Mode-locking threshold sets the limit on the maximum applied perturbation strength, but RFA can locally boost the internal perturbation field

$$\psi_{ext} \propto RFA\left(\beta/\beta_{crit}\right)^{a}\psi_{vac}$$

  - RFA ~ 3 is typical, increases quasilinear effects by x10!
- Improper interaction will couple to a global mode that will lock plasma rotation and cause disruption: best to avoid n=1, (n=2?)

- **If RFA is necessary in order to achieve the required perturbation strength for ELM control, then there is also threshold in beta**

$$\psi_{int} > \psi_{control} \rightarrow \beta > \beta_{control}$$

  - **But if beta is too large, ELMs will return, so there must be a window in beta**

$$\boxed{\beta_{ELM} > \beta > \beta_{control}}$$

Non-ideal physics near the rational surface $k_{||} = (m\text{-}nq)/qR \sim 0$ depends on key dimensionless #'s

- **Lundquist # S_L~10^9-10^{10} sets the basic resistive scales**
  - Balances inertia & resistance near rational surface

$$\tau_R = S^{1/3}\tau_H \sim 10^3\tau_H$$
$$\delta_R = S^{-1/3} r \sim 10^{-3} r$$

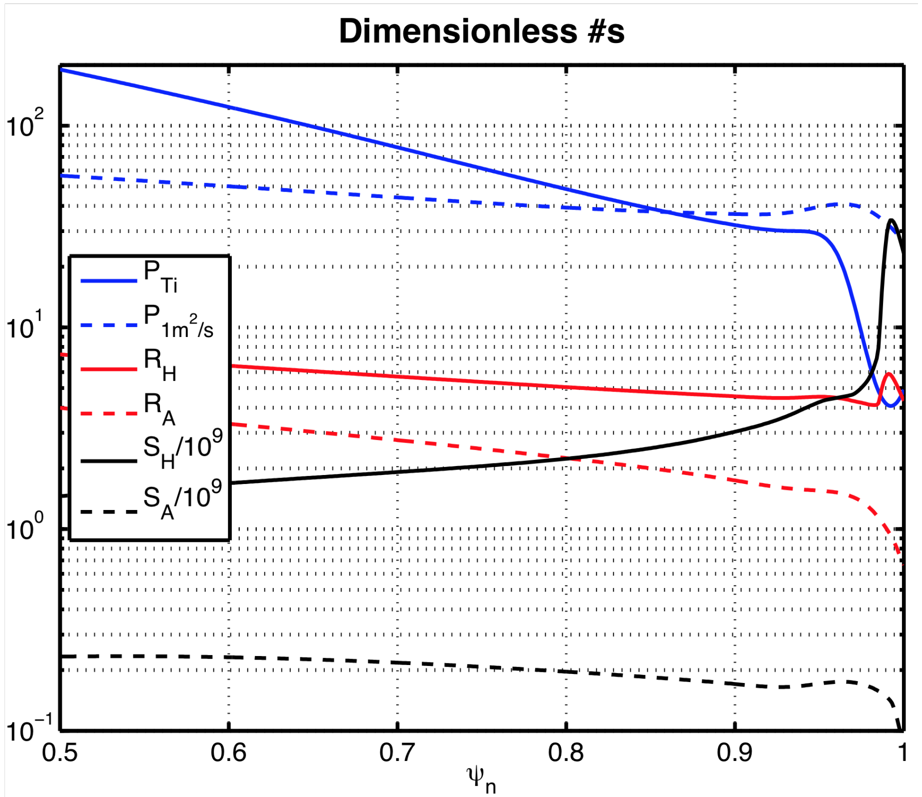

- **FLR effects are important!**
  - The resistive layer width is smaller than the gyroradius

$$\rho_\delta = \rho_s/\delta_R \sim 5-10$$

- **Even in H-mode, anomalous diffusivities are large!**
  - "Prandtl" numbers estimated from edge energy confinement time

$$P = \tau_R/\tau_{Viscous} \sim 10-100 \qquad D = \tau_R/\tau_{Diff} \sim 10-100$$

Fusion Energy Sciences

Diamagnetic flows within the H-mode pedestal steep-gradient region are larger than the ExB flows

- High-resolution experimental data & analysis techniques are needed to accurately measure flow velocities

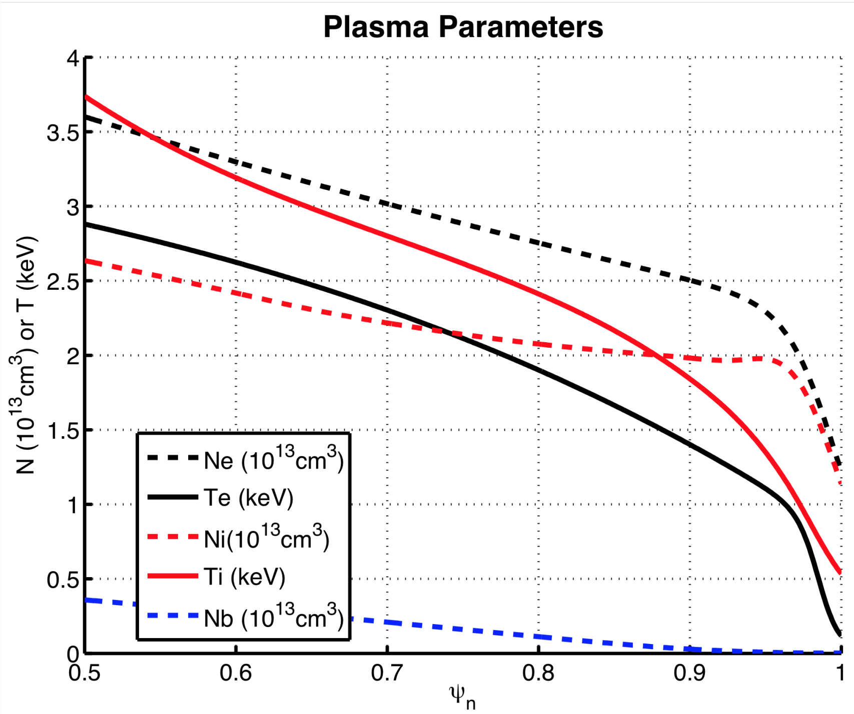

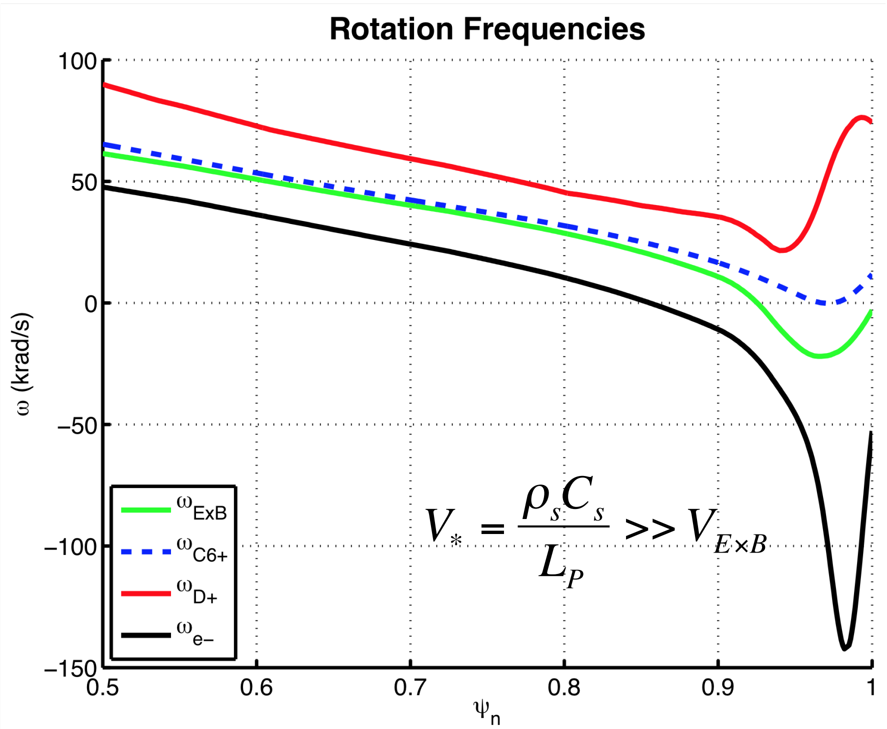

- **DIII-D 126006 in ELM suppression phase at 3600 ms**
  - Rotation frequency defined as an "equivalent" toroidal rotation

$$\omega_T \equiv \frac{\mathbf{k}_\perp \cdot \mathbf{V}}{n_{tor}} = \left(\omega_{tor} + q\omega_{pol}\right)$$

Drift-ordered models needed to capture FLR effects: 3-field model provides useful insight

- 1st order drift effects are described by the Hazeltine & Meiss[1] "flute-reduced" isothermal 4-field model[1]
  - d/dx >> d/dy >> d/dz
- Further assumption: low-beta → 3 field model
  - Eliminates parallel momentum equation, curvature terms
  - Good for top of pedestal, but toroidal geometry will couple surfaces together
  - Ohm's Law $$\frac{\partial\psi}{\partial t} = \nabla_{\parallel}\phi - \frac{\nabla_{\parallel}P_e}{en_e} + \eta J \qquad \frac{d}{dt} = \frac{\partial}{\partial t} + \frac{\mathbf{b}\times\nabla\phi}{B}\cdot\nabla$$
  - Vorticity $$\frac{dU}{dt} = V_A^2\nabla\cdot J_{\parallel} + \mu_a\nabla_{\perp}^2 U \qquad U = \nabla_{\perp}\cdot n_e\nabla_{\perp}\phi + \nabla_{\perp}^2 P_i$$ $$J_{\parallel} = \nabla_{\perp}^2\psi$$
  - Particle Cons. $$\frac{dn_e}{dt} = \nabla\cdot\frac{cJ_{\parallel}}{4\pi e} + \nabla\cdot D_a\nabla n_e \qquad P = n_e\left(T_e + T_i\right)$$
- Dispersion relation requires solving 8th order ODE
  - Can be reduced to 2nd order ODE after Fourier transformation from minor radius to ballooning angle & including effect of magnetic shear[2,3]

[1] Hazeltine & Meiss, Phys. Rep. **121**, 1 (1985)
[2] F.L. Waelbroeck, Phys. Plasmas **10**, 4040 (2003)
[3] A. Cole & R. Fitzpatrick, Phys. Plasmas **13**, 32503 (2006)

3-Field Model: Transmission factor has many different limiting forms depending on key dimensionless #'s: S_H, P, D, ρ_δ

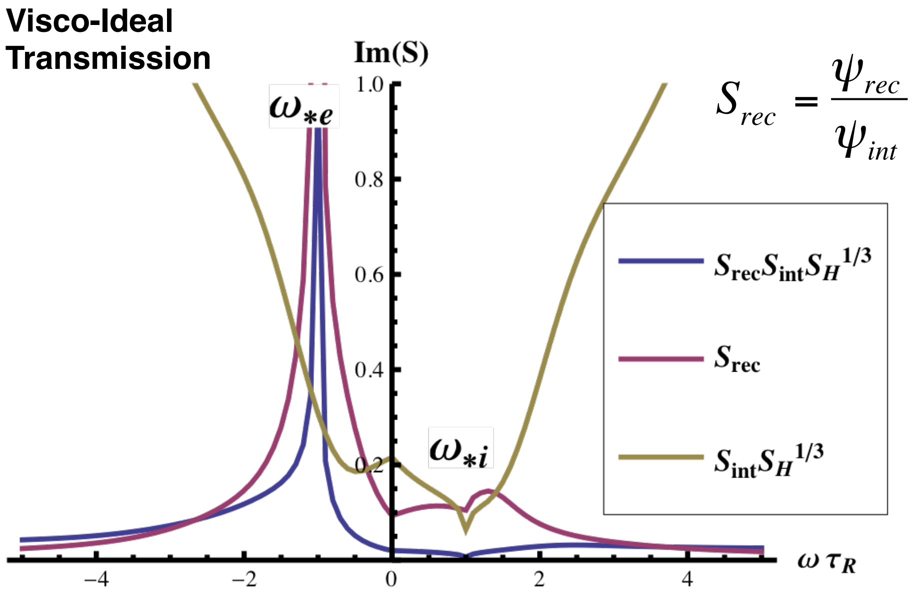

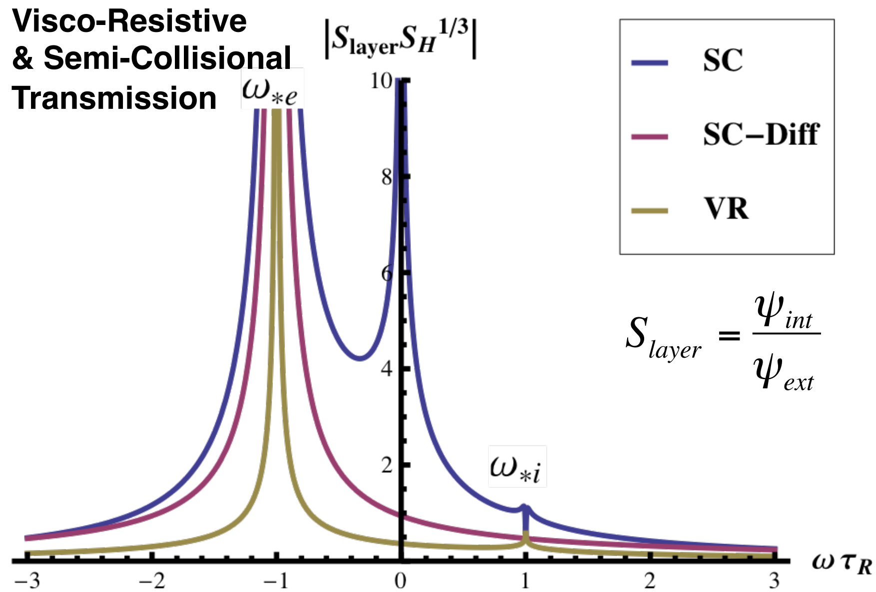

- Resonances occur near locations where: **V_{ExB}=0, V_i=0 and V_e=0**
  - Actual resonance locations are shifted by kinetic effects[1]
- Electron drift resonance appears in Visco-Resistive & FLR-regimes
  - Parallel Ohm's Law has resistance, but no impedance due to electron inertia
- Semi-collisional[2] regimes typically allows greater transmission
  - Diffusion tends to smooth ion and ExB resonances, but not electron resonance

[1]M.F. Heyn, et al. Nucl. Fusion **48**, 24005 (2008)

[2]J.F. Drake and Y.C. Lee, Phys. Fluids. **20**, 1341 (1977)

Experimentally, transmission is generally predicted to be small S~10^{-2}-10^{-3}, except in 2 places

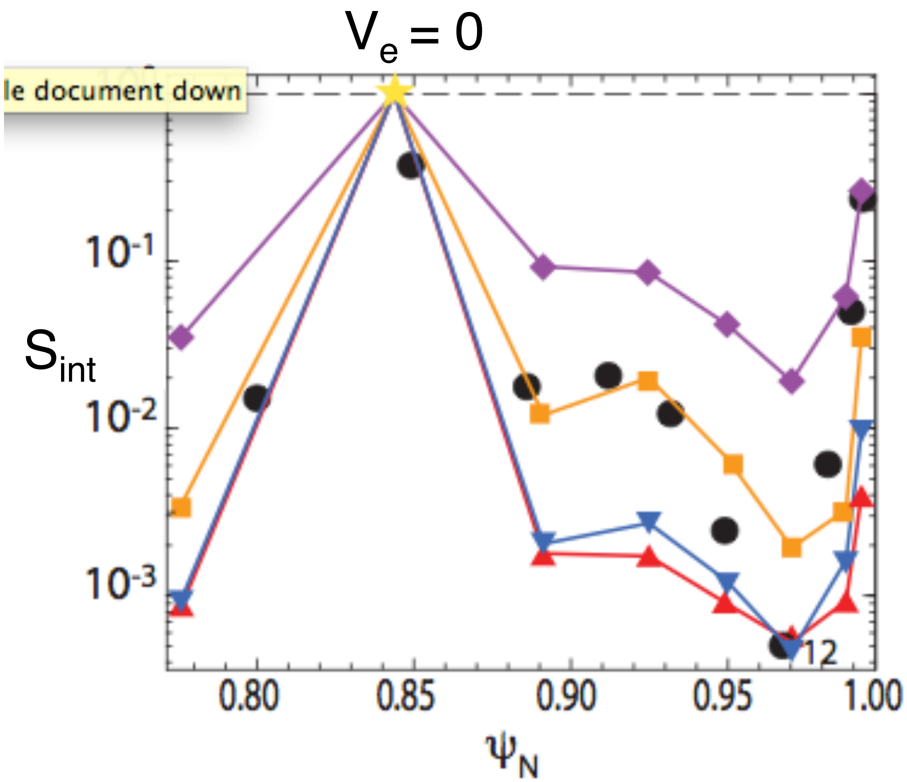

Analytic calculation of shielding by F.L. Waelbroeck

Examples: | **Equivalent to:**

Diamonds: MHD using $S_H/10^3$ — Nonlinear code

Triangles: MHD μ=0.01 m^2/s — Linear code

Triangles: 2-fluid μ =1 m^2/s — Theory

Squares: 2-fluid μ=0.01 m^2/s — Theory

Circles: linear kinetic calculation[1]
- -Coulomb collisions via Krook operator
- -no anomalous diffusion

[1]M. F. Heyn, et al. Nucl. Fusion (2008)

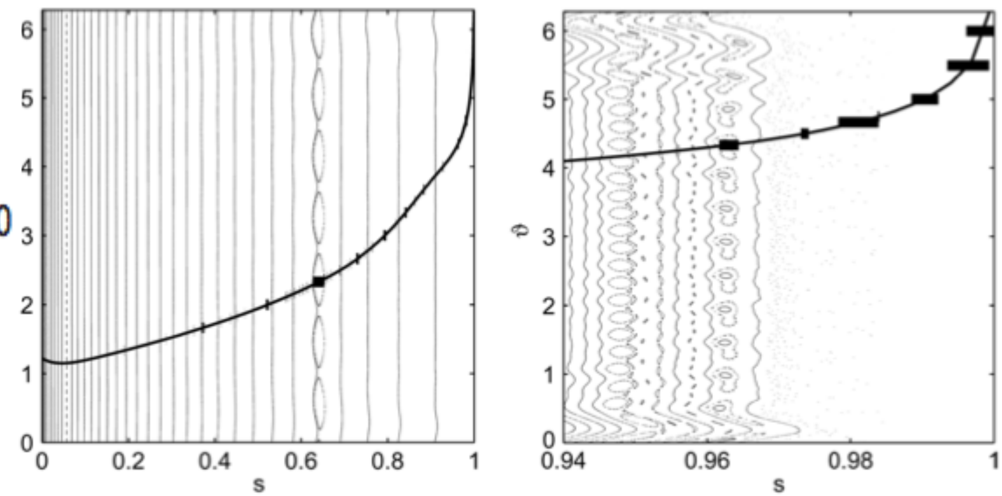

1. At the electron resonance V_e=0

2. At the FOOT of the pedestal, where the plasma is extremely cold

Significant reconnection only occurs for ψ > 99%

OUTLINE

- Motivation
- Plasma Response to Applied Fields
- Transport Mechanisms
  - Ambipolarity constraint
  - Stochastic transport?
- Small-Island transport
- Conclusions

Which transport mechanism governs the particle pumpout?

- Particle transport equations

$$\partial_t n_e = -\nabla\cdot n_e\left(V_\parallel + V_E + V_{*p,e} + V_{2,e}\right) + \nabla\cdot J/e$$

$$\partial_t n_i = -\nabla\cdot n_i\left(V_\parallel + V_E + V_{*p,i} + V_{2,i}\right)$$

$$V_E = \frac{b}{eB}\times\nabla\phi$$

$$V_{*p} = \frac{b}{enB}\times\nabla p$$

$$nV_2 = \nabla_\perp\cdot\frac{mn}{B}\partial_t\nabla_\perp\phi + \frac{b}{eB}\times(\nabla\Pi + R)$$

- Ambipolar transport processes: 2D & 3D
  - Axisymmetric neoclassical transport
  - Convective transport: parallel flow $V_{||}$, turbulent transport V_E

- Non-ambipolar transport processes: 3D
  - Free-streaming along field lines is not ambipolar since V_{te}>>V_{ti}
  - Collisional transport is not intrinsically ambipolar in 3D fields since ρ_i>>ρ_e

- Criterion for observation within experiment Γ_{RMP}~ $\Gamma_{pedestal}$ or D_{RMP} ~ $D_{pedestal}$
  - Typically $D_{pedestal}$ ~ D_{neo} ~ 0.1-0.4 m^2/s
  - Increasing turbulent diffusivity by x 2-3 could do the trick

Non-ambipolar transport actually requires 2 mechanisms: need enhancement in both electron and ion channels

- Ambipolarity requires electron & ion transport to balance

$$0 = \nabla\cdot J = \nabla\cdot\left(J_{\parallel} + J_{*p} + J_{pol,e}\right) = \nabla\cdot\left(J_{\parallel} + en_e\left(V_{*p,i} + V_{2,i} - V_{*p,e} - V_{2,e}\right)\right)$$

- Since ion & electron transport proportional to free energy, a radial electric field arises to balance the flows
  - General transport relations

$$J_e = \sigma_e\left(E_e - E\right)$$

$$J_i = \sigma_i\left(E - E_i\right)$$

$$\frac{eE_i}{T_i} = \frac{dn_i}{dr} + k_{ii}\frac{dT_i}{dr}$$

$$\frac{eE_e}{T_e} = -\frac{dn_e}{dr} - k_{ee}\frac{dT_e}{dr} - k_{ei}\frac{dT_i}{dr}$$

Ambipolar electric field & flux

$$E_A = \frac{\sigma_e E_e + \sigma_i E_i}{\sigma_e + \sigma_i}$$

$$J_A = J_i = -J_e = \frac{E_e - E_i}{1/\sigma_e + 1/\sigma_i}$$

- Transport is slowed to the rate determined by the smallest conductivity
  - If either σ_i or σ_e vanishes, the transport vanishes $\Gamma=\Gamma_A=0$ once $E=E_A$

The transport mechanisms must have the right magnitude – including the estimate of the transmission factor

- Stochastic transport – electron channel
  - $D_e \sim qRV_{te}\,(\delta B_{vac}/B)^2 \sim 10\text{-}100\ m^2/s$ ← Too large (OK for particles, not heat)
  - $D_e T_{rec} \sim 0.01\text{-}0.1\ m^2/s$ ← Too small (no stochasticity)

- Viscous drift transport – ion channel
  - Axisymmetric neoclassical[1] $D_{plateau} \sim \rho^2 V_t/qR \sim 0.1\text{-}1 m^2/s$ ← Just right
  - Non-axisymmetric neoclassical[2] $D_{na} \sim \rho_p V_t\,(\delta B_{tot}/B)^2\, S^2_{ext} \sim 0.01 m^2/s$ ← Too small?

- Transport within an isolated island must balance || transport and viscous drift
  - $D_B \sim \rho V_t/\beta\,(\delta B_{vac}/B)^2 \sim 0.01\text{-}0.1\ m^2/s$ ← OK?
  - $D_B S_{int} \sim 0.001\text{-}0.01\ m^2/s$ ← Too small (islands must open for effect)

[1]M.Z. Tokar, et al., Phys. Plasmas **15** (2008) 072515
V. Rozhansky, et al., Nuclear Fusion **50** (2010) 034005

[2]K.C. Shaing, et al., Nuclear Fusion **50** (2010) 025022
J.K. Park, et al., Phys. Rev. Lett. **102** (2009) 065022

Can stochastic field line transport explain the reduction in edge pressure gradient?

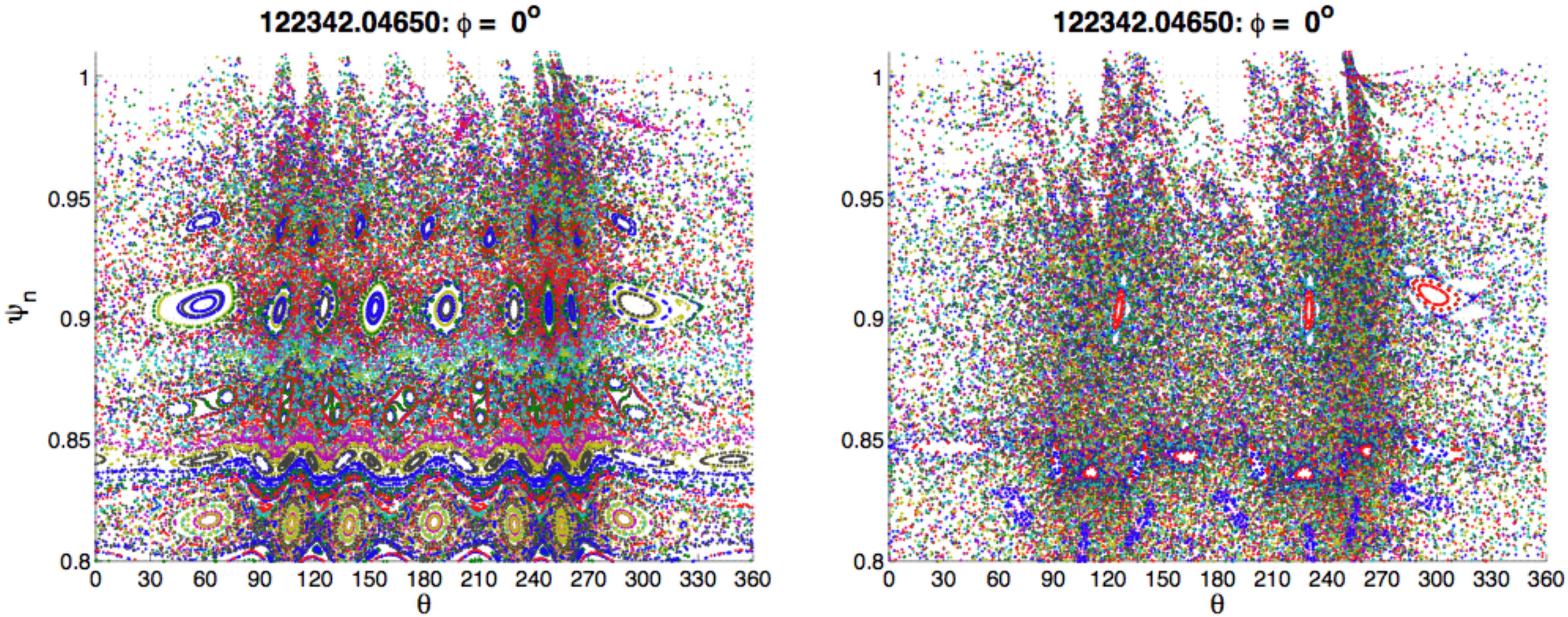

I-coil only: slow diffusion ***I-coil + C-coil + field error: rapid loss***

- **Original working hypothesis of the DIII-D ELM-control team:**
  "Perturbations induce magnetic diffusion and fractal structure in the edge"

- TRIP3D code superimposes external coil fields & Grad-Shafranov EFIT equilibrium
  Plasma is treated as a resistive "vacuum" instead of as an ideal conductor

Stochastic particle motion generates macroscopic diffusion of the fluid moments of the plasma[1,2]

- Particle conservation

$$\partial_t n + \nabla \cdot nV = -\nabla \cdot \Gamma_{st}$$

$$\Gamma_{st} = -\frac{D_{st}}{T} \cdot \left(T\nabla n + ZenE + \frac{1}{2} n\nabla T \right)$$

- Energy conservation

$$\partial_t \frac{3}{2} nT + \nabla \cdot \frac{3}{2} nTV + nT\nabla \cdot V = -\nabla \cdot Q - \nabla \cdot Q_{st} - ZeE\Gamma_{st}$$

$$Q_{st} = -2D_{st} \cdot \left(T\nabla n + ZenE + \frac{3}{2} n\nabla T \right)$$

- Numerical factors reflect the dependence of diffusion on the parallel speed $|v_{||}|$

- The ensemble averaged diffusion coefficient is defined by the average speed

$$D_{st} = d_{\mathrm{fl}} \sqrt{\frac{2T}{\pi m}} \qquad d_{\mathrm{fl}} \approx \pi qR \sum_n \left(\frac{\delta B}{B} \right)^2_{m=qn}$$

[1]A.B. Rechester and M.N. Rosenbluth, Phys. Rev. Lett. **40** 38 (1978)
[2]R.W. Harvey, et al., Phys. Rev. Lett **47** 102 (1980)

Parallel transport is not ambipolar and an electric field must develop to restore ambipolarity[1]

- Electron diffusion is much more rapid than ion diffusion

$$D_{st,e}/D_{st,i} = V_{th,e}/V_{th,i} = \sqrt{m_i/m_e} \sim 60$$

- The only way to achieve ambipolarity $\Gamma_{st,e} = \Gamma_{st,i}$ is if the free energy that drives electron diffusion almost vanishes

$$\Gamma_{st,e} = \frac{D_{st,e}}{T}\left(T\nabla n - enE + \frac{1}{2}n\nabla T\right) \approx 0$$

- The non-ambipolar flux sets the ambipolar electric field $eE_{st} = \left(T_e\frac{\nabla n_e}{n_e} + \frac{1}{2}\nabla T_e\right)$

- Both particle fluxes now diffuse at the slower ion diffusion rate

$$\Gamma_{st} = \nabla\cdot n_e D_{st,i}\cdot\left(2\frac{\nabla n_e}{n_e} + \frac{1}{2}\left(\nabla T_i + \nabla T_e\right)\right)$$

- Thermal conduction times scales are very different for each species
  - "*Rechester-Rosenbluth*" electron conduction $\qquad Q_{st,e} = 2D_{st,e}\cdot n_e\nabla T_e$
  - Ions respond to total pressure $\qquad Q_{st,i} = D_{st,i}\left(2\nabla\left(p_i + p_e\right) + n_e\nabla\left(T_i - T_e\right)\right)$

[1]T. Stix, Nucl. Fusion **18** 373 (1978)
[2]R.W. Harvey, et al., Phys. Rev. Lett **47** 102 (1980)

Quasilinear thermal diffusivity estimates are too high to match experimental results – considering I-coil alone[1]

Collisionality

$$\lambda_* = \lambda_{mfp} / L_K$$

Quasilinear field line diffusion

$$d_{\mathrm{fl}} = \pi q R \sum_n \left(\frac{\delta B}{B} \right)^2_{m=qn}$$

Collisionless diffusion

$$D_{st} = d_{\mathrm{fl}} V_T$$

Collisional diffusion

$$D_{\mathrm{RR}} = D_{\mathrm{st}} \lambda_{mfp} / L_{\mathrm{T}} = D_{||} d_{\mathrm{fl}} / L_{\mathrm{T}}$$

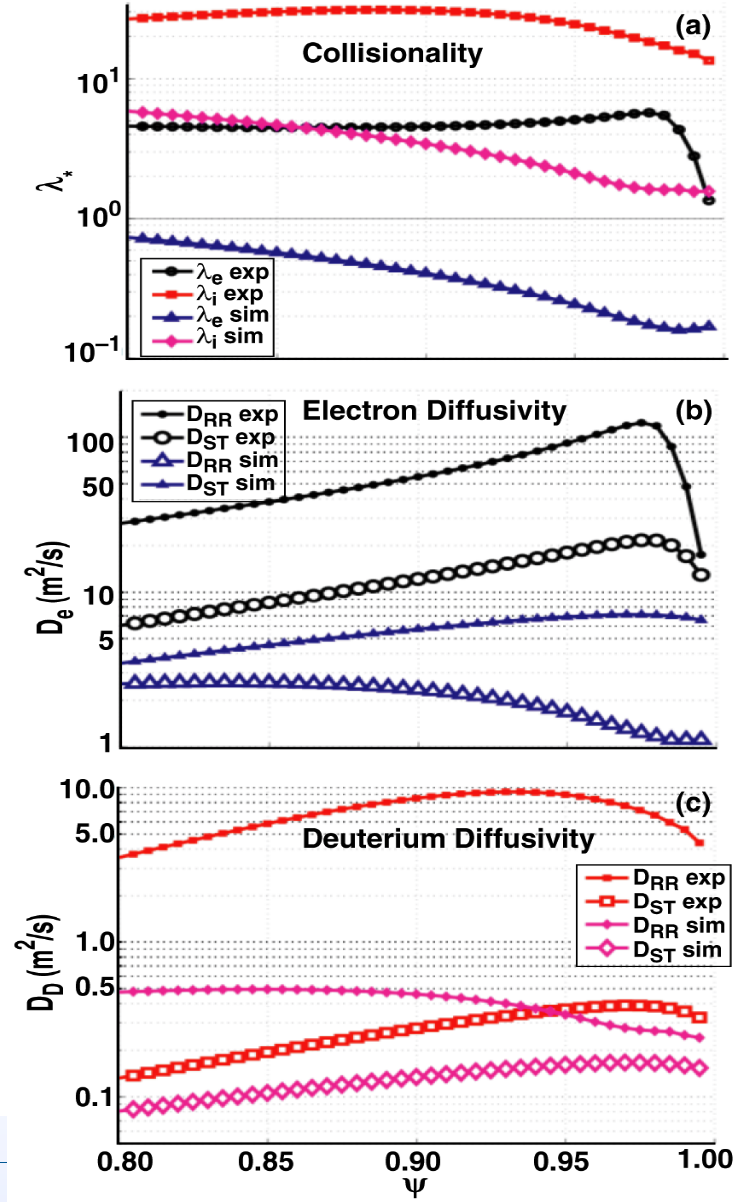

[1]I. Joseph, et al., Nucl. Fusion **48** 045009 (2008)

Pedestal cools as stochastic layer increased

I-coil (kA):

0 (axisymmetric) ***1*** ***2*** ***3***

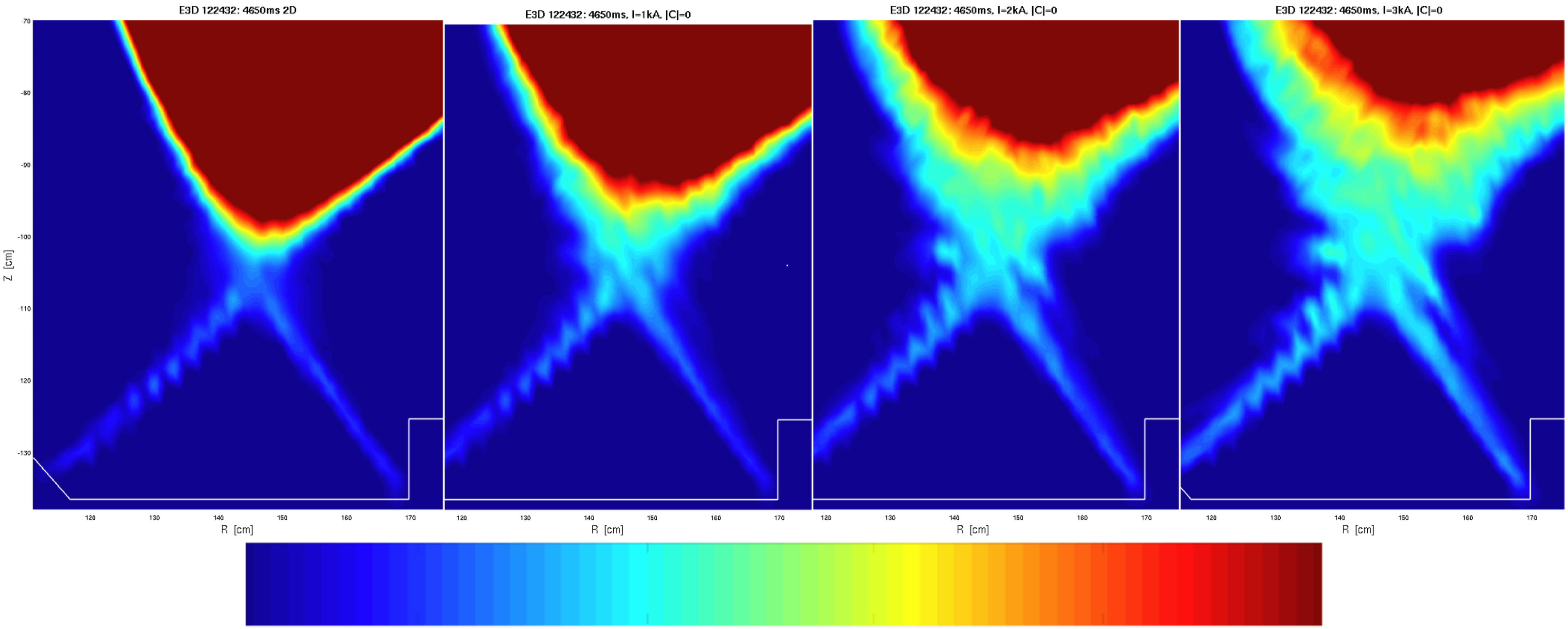

Te (eV): *50* *100* *150* *200*

$$D_{\perp} = 0.2 m^2 / s \quad n_{sep} = 4 \times 10^{18} m^{-3}$$

[1]I. Joseph, et al., J. Nucl. Mater. **363-365** 591 (2007)

Te and Ti predicted to be strongly reduced by stochastic field line diffusion

No transport barrier D = 1 m²/s constant heat flux BC's

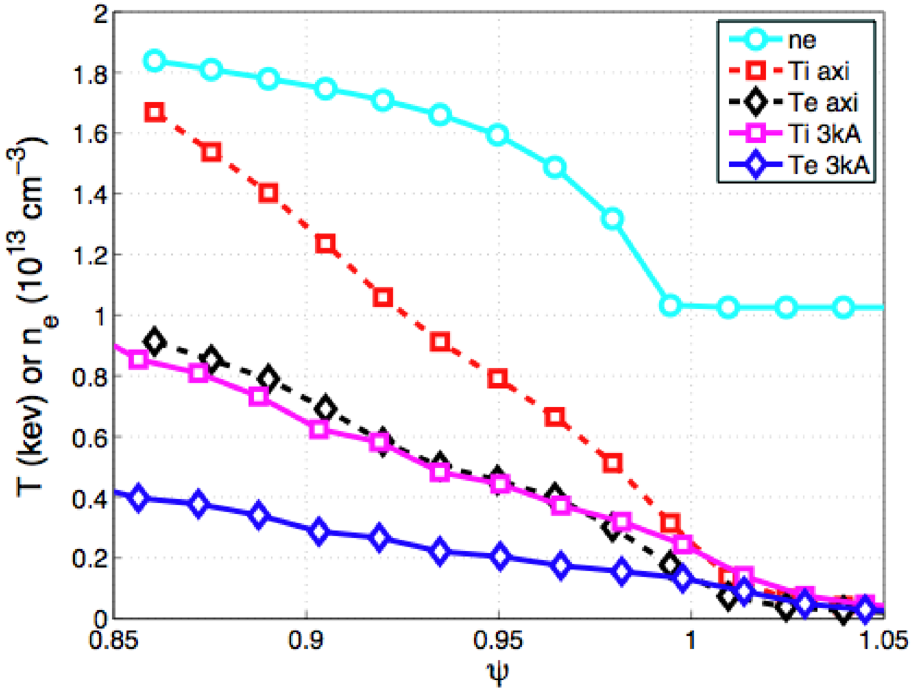

I-coil scan at D = 0.2 m²/s constant temp BC's

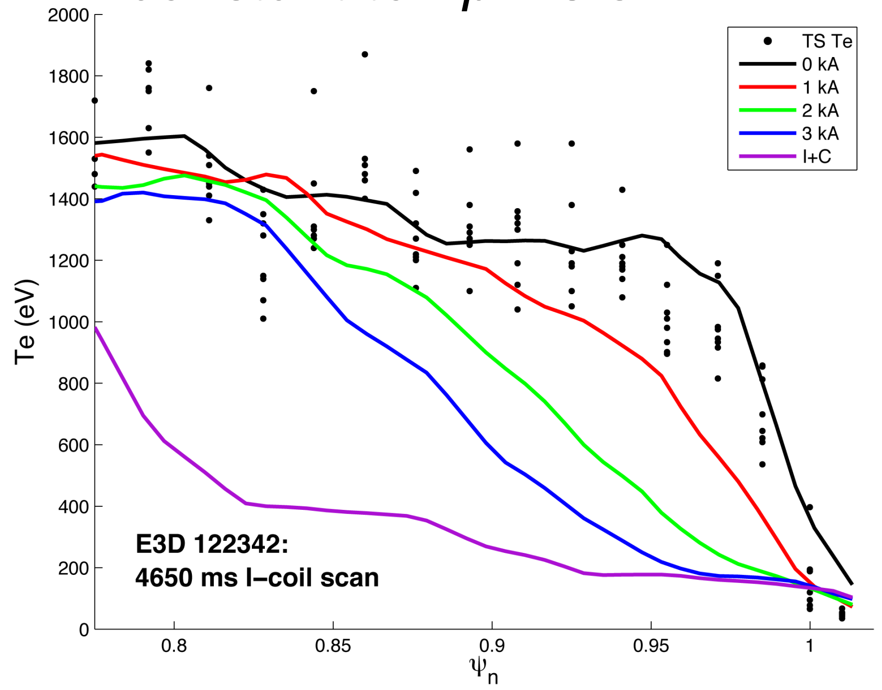

- n_e assumed to be a flux function
- Thermal transport increases as expected

In fact, the edge rotation is measured to spin up, not down!

- Edge impurity (CVI) and inferred ion toroidal rotation are found to increase in the edge region

- E_r does become more positive, but not in agreement with stochastic ambipolar field
  - XGC0 calculation by G.Y. Park

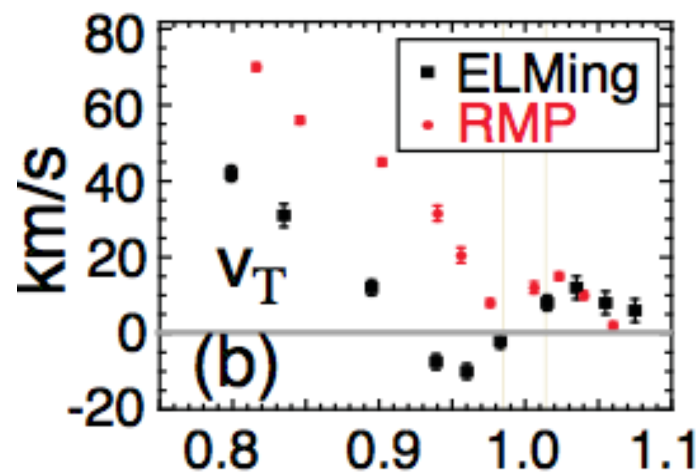

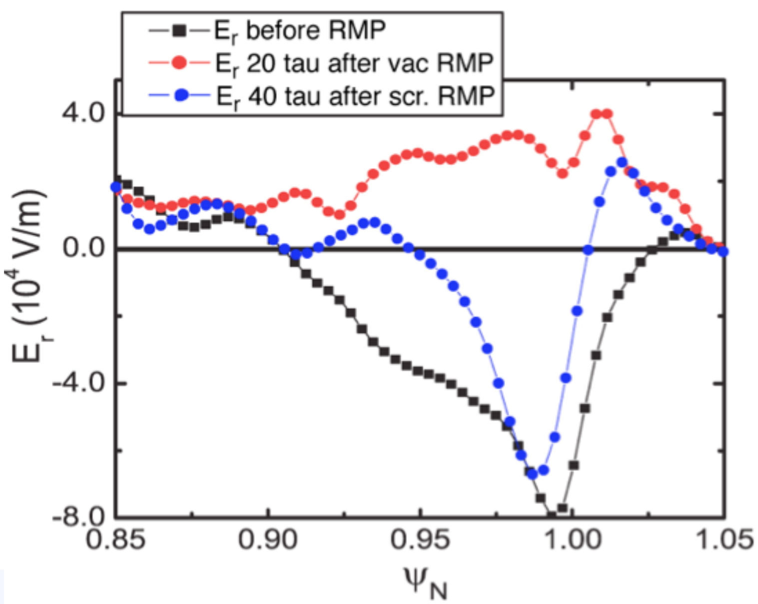

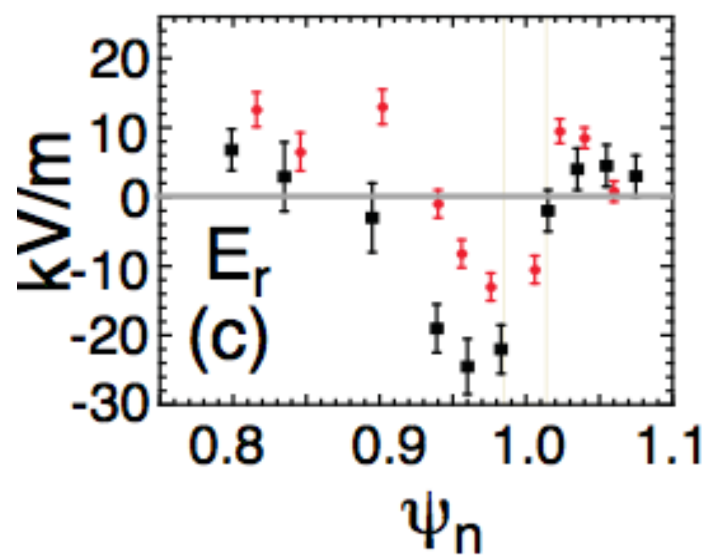

Outer strike-point develops pronounced non-axisymmetric strike point structure

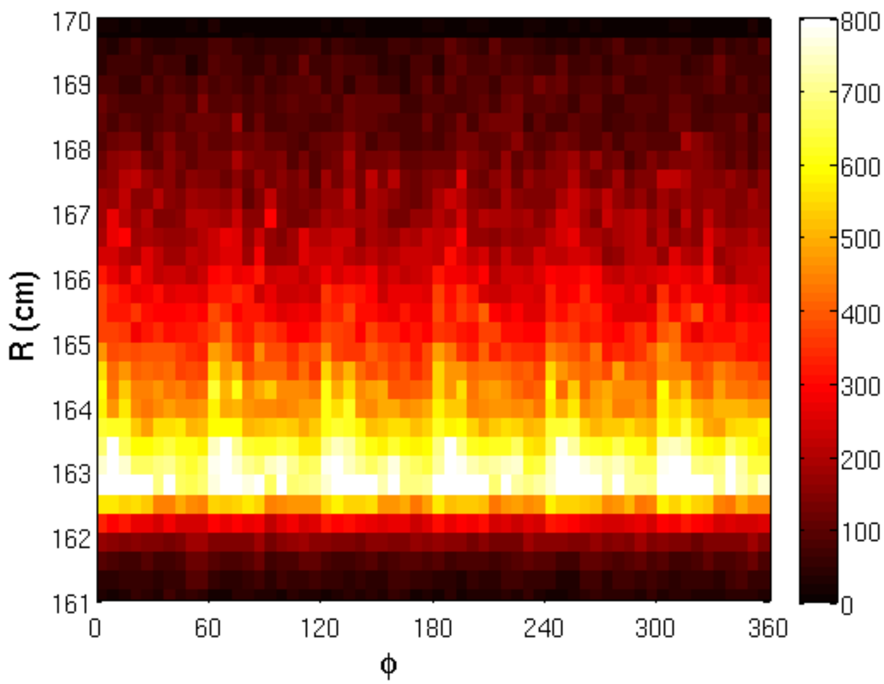

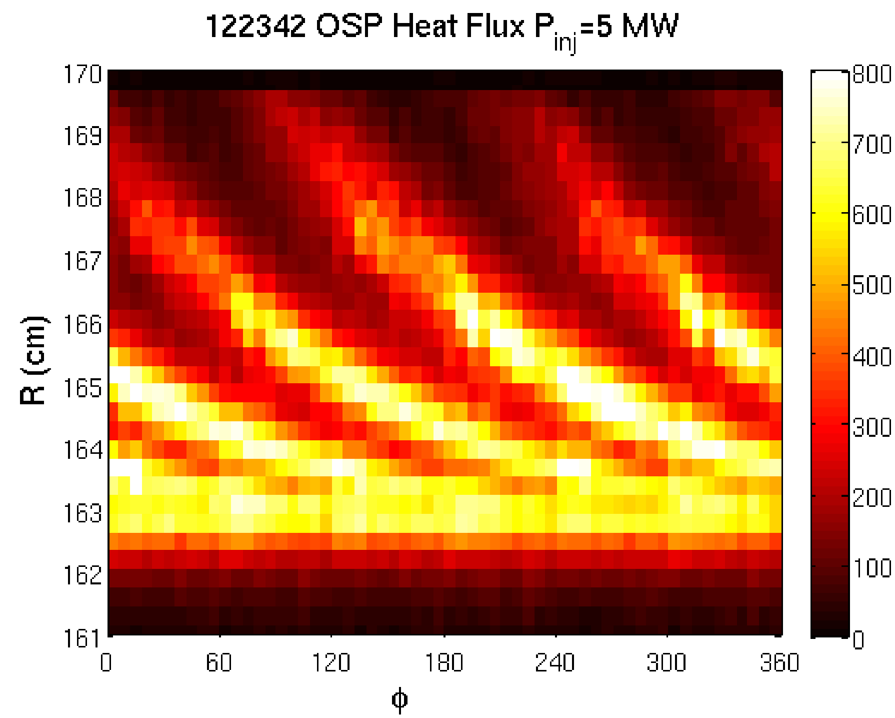

- Heat flux delivered to regions of long connection length

- Verification of thermal footprint allows verification of magnetic field structure

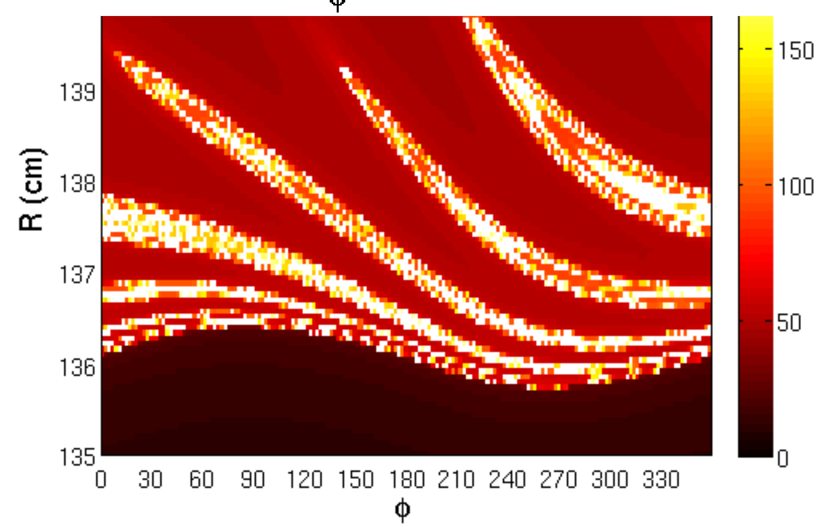

Multiple striation were observed in particle flux!
Is this caused by RMP magnetic footprint structure?

- 5 cm width qualitatively matches TRIP3D field line tracing

- Width scales as ~ $(\delta B/B)_{res}$

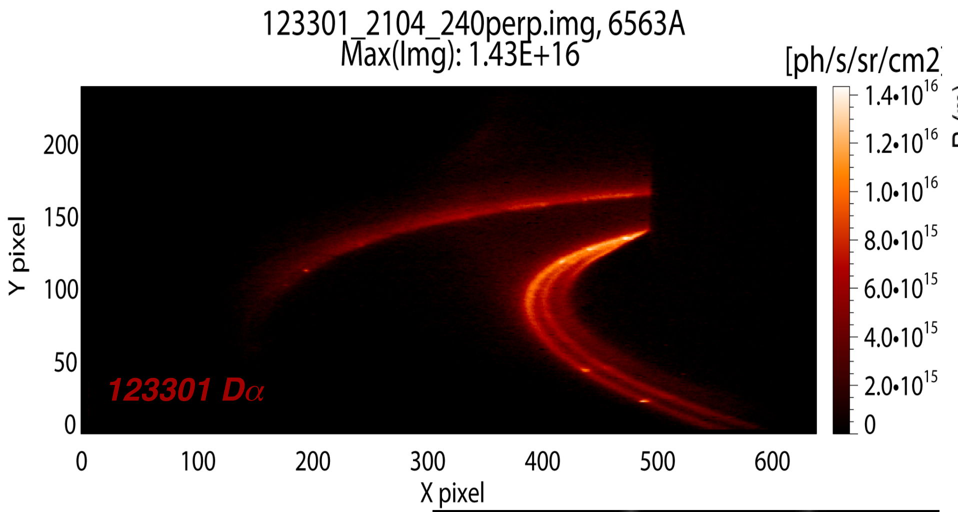

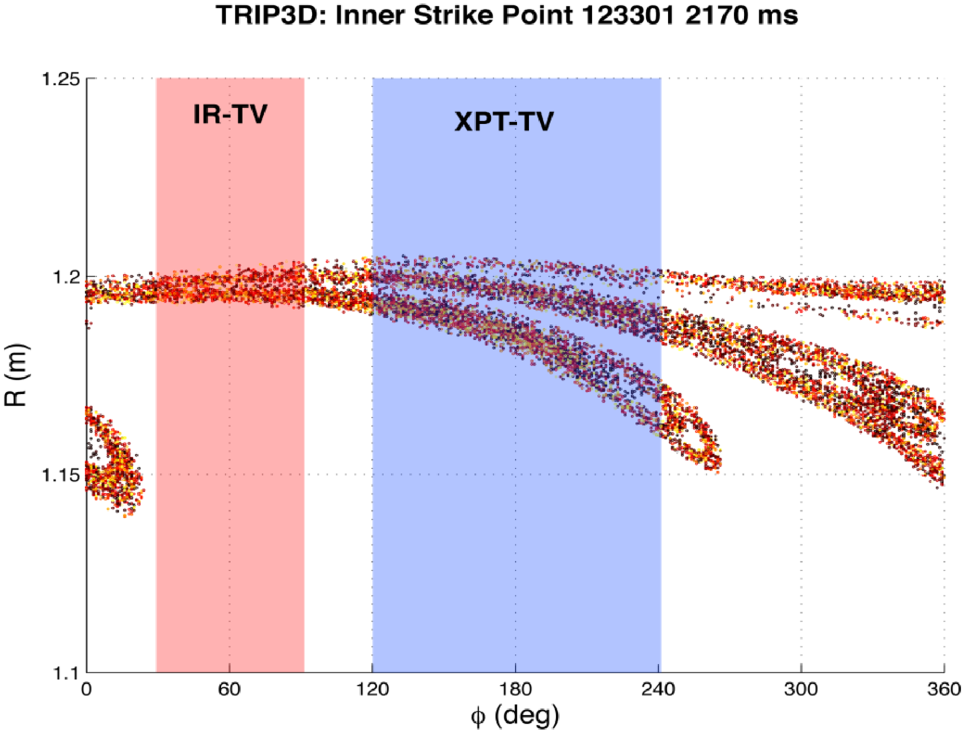

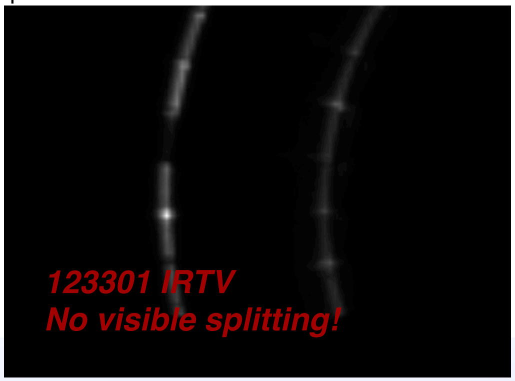

- Heat flux striations were not observed at 60° IR camera location

- Inspired additional IR camera at a location of 160°

However, measured heat & particle fluxes are quite different!

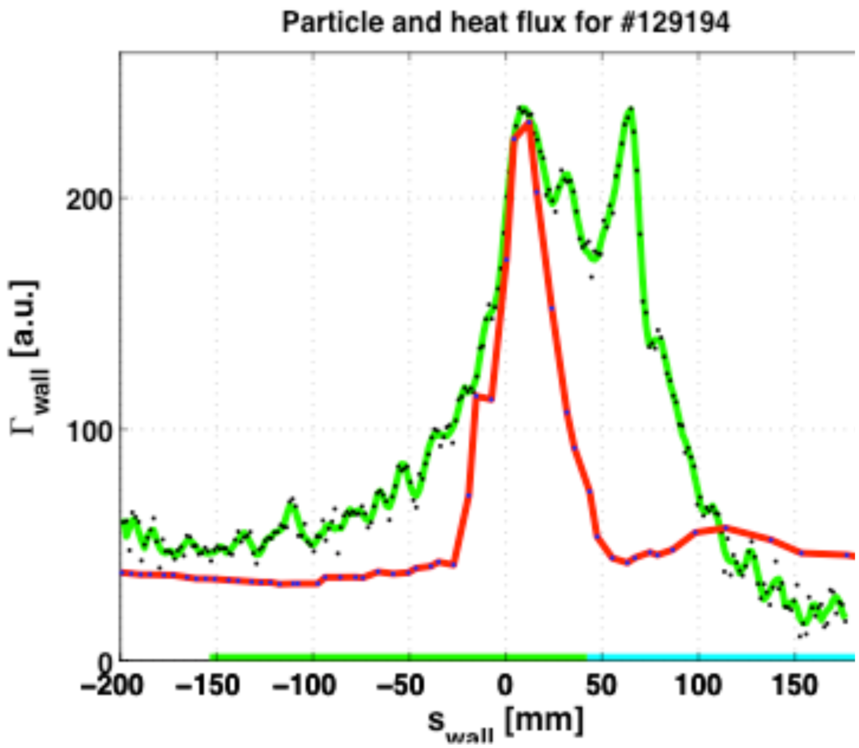

129194 ISP 3.0-3.2 sec

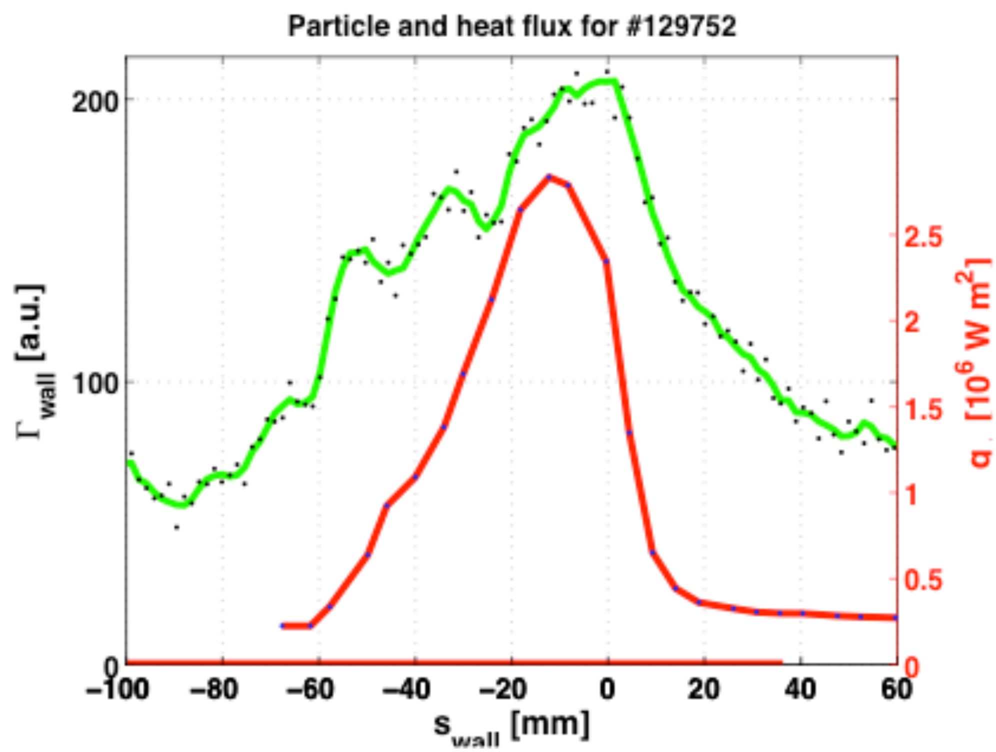

129752 OSP 3.2-3.6 sec

- Heat flux is axisymmetric
  - **TEXTOR IR camera placed near 160°**
  - **Neither IR camera shows significant strike point splitting**
- DIMEs camera (filtered Dα) also near 160°

  (M Jakubowski & O Schmitz, FZ-Julich)

OUTLINE

- Motivation
- Plasma Response to Applied Fields
- Transport Mechanisms
- **Small-Island transport**
  - Magnetic flutter transport balances viscous transport
  - Drift wave radiation by magnetic islands
  - Shear flow damping by additional viscous forces
- Conclusions

Quasilinear Lorentz Force: generated by screening current and perturbed magnetic field

- Average Lorentz force density
  - Large at rational surfaces
  - Proportional to transmission factor S_{layer}

$$\mathbf{f}_{ql} = \frac{\oint \mathbf{J}\times\mathbf{B}\,d^2a}{A_{surf}} = \frac{d}{dx}\frac{\langle [B_x B_y] \rangle}{4\pi}\hat{\mathbf{k}}_\perp$$

$$f_{ql} = \frac{|B_x|^2}{4\pi}\delta(x)\,\mathrm{Im}\frac{\Delta_{layer}}{2k_\perp} = \frac{|B_{ext}|^2}{4\pi}\delta(x)\,\mathrm{Im}\,S_{layer}$$

- The perpendicular force is large, but the poloidal component is balanced by poloidal flow damping, leaving only the smaller toroidal component
  - For experimental conditions with $B_{\mathrm{ext}} \sim 6$ G
  - $F_{\mathrm{ql}} = \int d^3x\, f_{\mathrm{ql}} \sim 10$ N x Im S_{layer} while $F_{\mathrm{tor}} = \int d^3x\, f_{\mathrm{ql}}\, B_{\mathrm{pol}}/B \sim 1$ N x Im S_{layer}

- In equilibrium, the toroidal component must be balanced by another force
  - **Anomalous viscosity leads to a cusp in V_{tor}**
  - $[dV_{\mathrm{tor}}/dx] \sim 200$ krad/s x Im S_{layer}

$$MN\partial_x \mu_a \partial_x V_{tor} = -\frac{B_{pol}}{B} f_{ql}$$

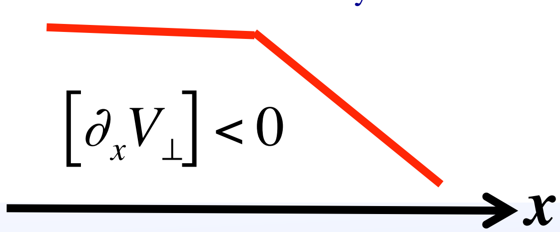

$$\boxed{\mu_a [\partial_x V_{tor}] = -\frac{V_A^2}{2}\frac{B_{pol}}{B}\left|\frac{B_{ext}}{B}\right|^2 \mathrm{Im}\,S_{layer}}$$

Quasilinear magnetic flutter flux due to $J_{||}$ along perturbed field lines $\delta B_{\perp}$

- "Magnetic flutter flux" is the ambipolar || electron flux = perp. ion flux
  - Large at rational surfaces

$$\Gamma_B = \frac{\int \mathbf{J}_{||} \cdot d^2 a}{eA_{surf}} = \frac{d}{dx} \frac{\left\langle \left[B_x B_y \right] \right\rangle}{4\pi e B / c}$$

$$= \frac{N V_A^2}{\omega_{ci}} \delta(x) \left| \frac{B_{ext}}{B} \right|^2 \operatorname{Im} S_{layer} = D_B N \delta(x)$$

- Flutter flux residue yields a "diffusion"
  - However, can point inward or outward depending on the sign of S_{layer}

$$D_B = \frac{\rho V_{th}}{\beta} \left| \frac{B_{ext}}{B} \right|^2 \operatorname{Im} S_{layer}$$

- For experimental conditions with $B_{\text{ext}} \sim 6$ G
  - $(dN/dt)_{\text{ql}} = \int d^3x\, \Gamma_{\text{B}} \sim 2\text{x}10^{19}/\text{s} \text{ x } \operatorname{Im} S_{\text{layer}}$

- In equilibrium, the flutter flux must be balanced by another flow
  - **Anomalous diffusion leads to a jump in N**
  - $[N]/N \sim 10\% \text{ x } \operatorname{Im} S_{\text{layer}}$

$$D_a \partial_x N = -\Gamma_{ql}$$

$$\boxed{\frac{[N]}{N} = -\frac{D_B}{D_a}}$$

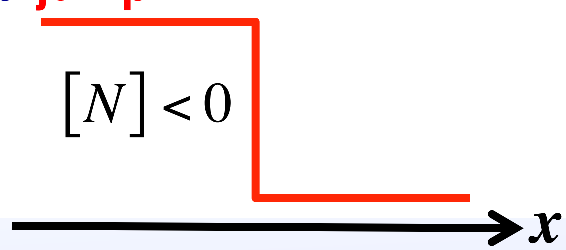

If anomalous diffusivities determine the equilibrium state, then the QL Flux is proportional to the QL Force

- Eliminating $|B_{ext}/B|^2$ leads to

$$\boxed{\frac{[N]}{N} = \frac{\mu_a}{D_a} \frac{\rho_{pol}[\partial_x V_{tor}]}{V_{th}}}$$

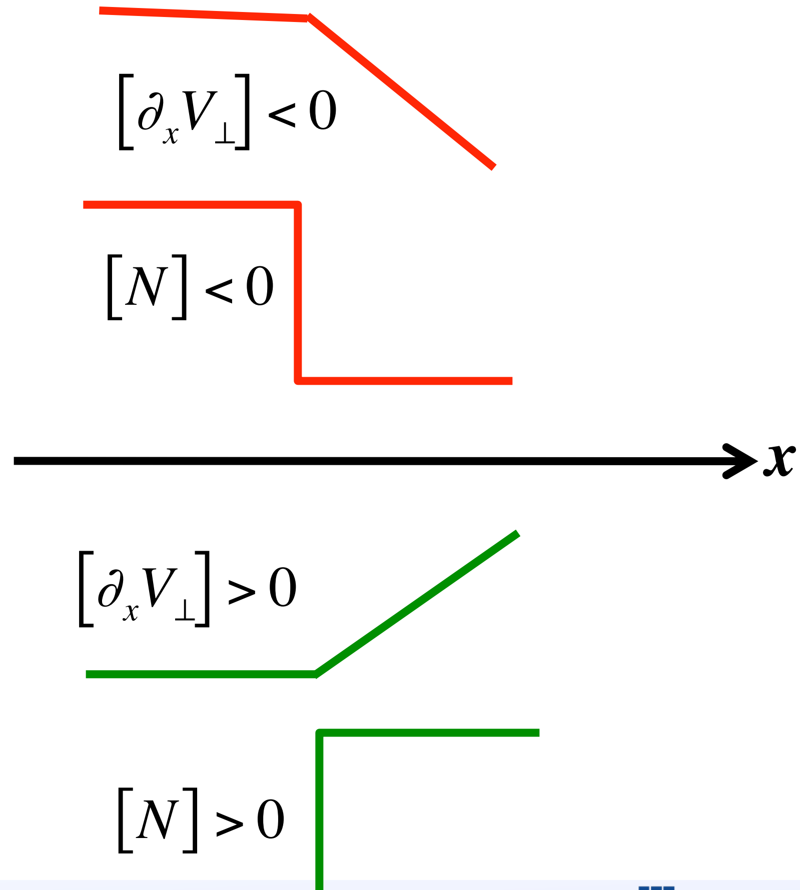

- F_B can brake the ion rotation while
  Γ_B generates an inward pinch
  - only possible single fluid result

- F_B can accelerate the ion rotation while
  Γ_B generates outward exhaust
  - possible in two-fluid regimes

In the region where electrons & ions rotate in opposite directions, ions accelerate and the flux points outward

- **This qualitatively matches two critical experimental observations**

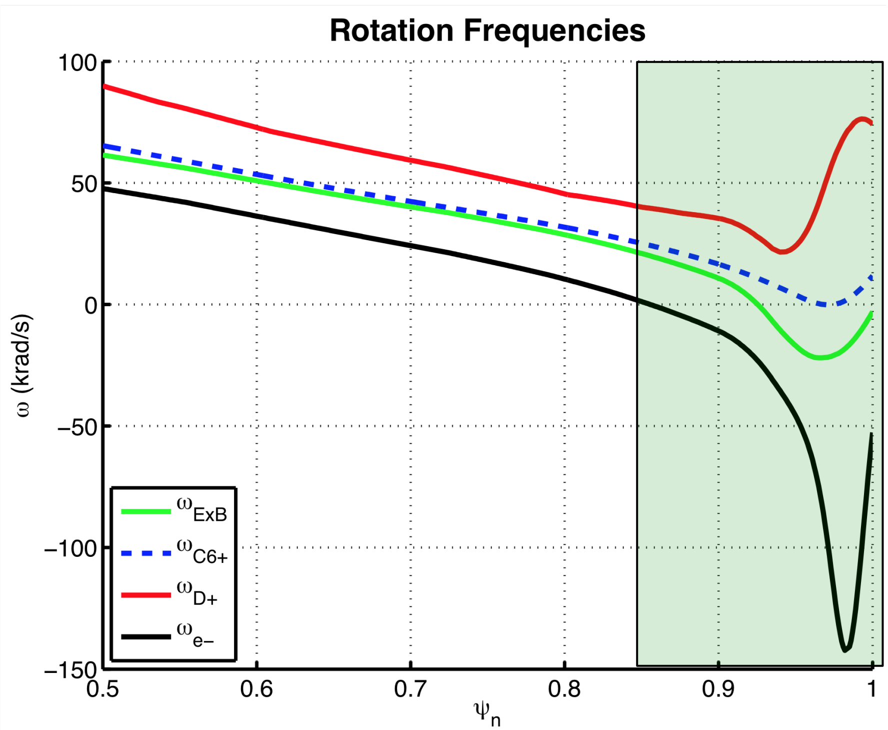

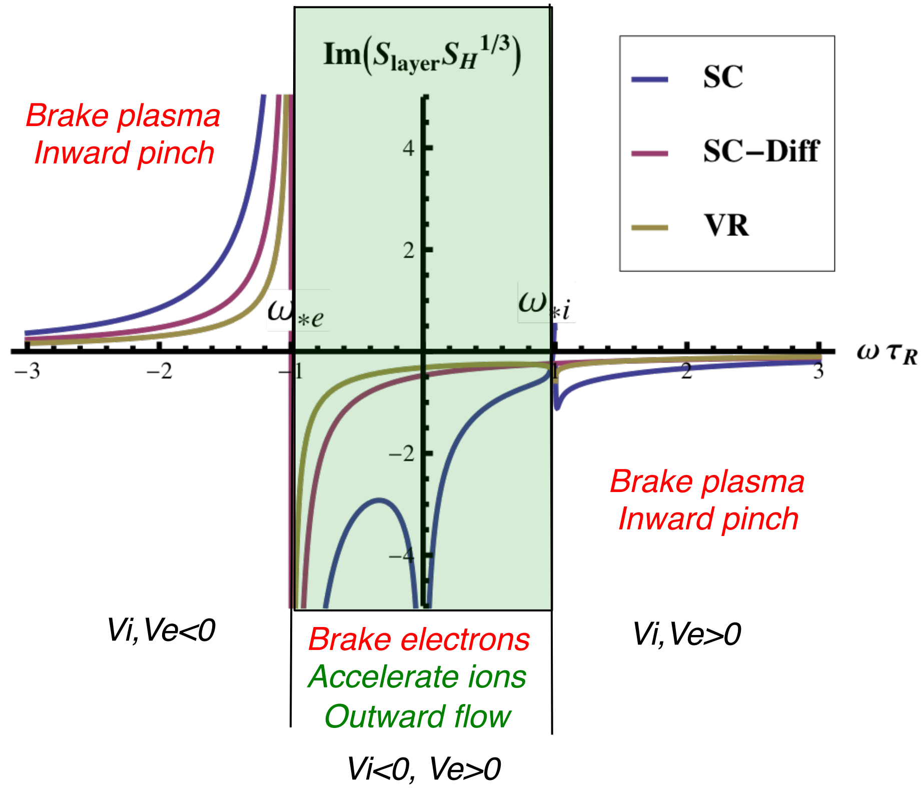

  – Im S_{layer} determines both magnitude and the direction of the force & flux

$$S_{layer} = \frac{\psi_{int}}{\psi_{ext}}$$

Convective transport: Drift waves can be radiated by islands whose widths are on the order of the ion gyroradius[1]

- At large distances, the equilibrium density profile must follow the Maxwell-Boltzmann relation ***modulo a flux function***
  - Flux function must yields correct density gradient at large x

$$\log(n_e) = \frac{e\phi}{T_e} + \frac{w}{L_n}\left(1 - \frac{\omega_0}{\omega_*}\right)h(\psi) \qquad \psi = \frac{1}{2}\left(\frac{x}{w}\right)^2 + \cos(k_y y - \omega t)$$

$$\lim_{x\to\infty}\log(n_e) = \frac{x}{L_n} \qquad h(\psi) = \sqrt{2(\psi - 1)} \times \Theta(\psi - 1)$$

- **Sharp structure in density profile acts as a source of drift waves[1]**

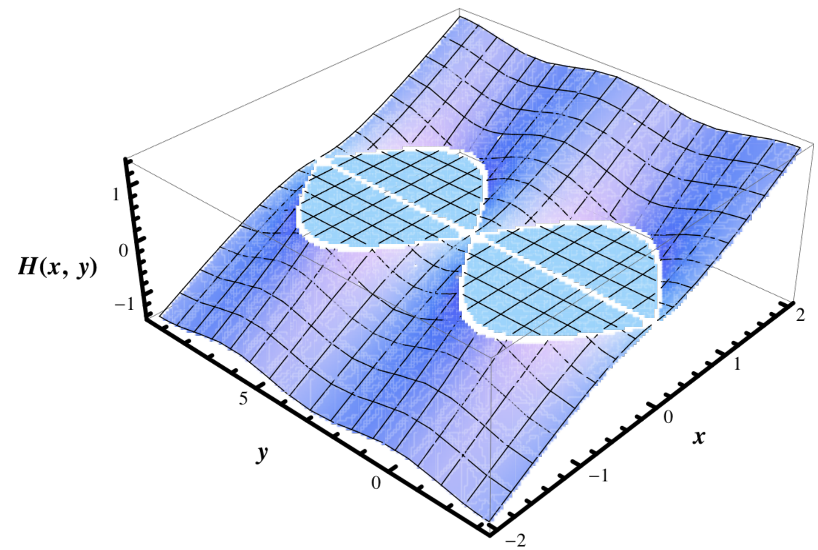

[1]Waelbroeck, et al., Phys. Rev. Lett. **87** (2001) 215003
R. Fitzpatrick and F.L. Waelbroeck, Phys Plasmas **12** (2006) 122511
F. Mililtello and F. L. Waelbroeck, **49** Nucl. Fusion (2009) 065018

Radiated flux can be calculated within 3-field model

- **Collisional isothermal drift wave model including magnetic shear**

$$\frac{dn_e}{dt} - D_a \nabla_\perp^2 n_e = \rho^2 \left(\frac{dU}{dt} - \mu_a \nabla_\perp^2 U \right)$$

$$\frac{d}{dt} = \frac{\partial}{\partial t} + \frac{\mathbf{b} \times \nabla \phi}{B} \cdot \nabla$$

$$U = \nabla_\perp^2 (\phi + P_i)$$

$$J = \nabla_\perp^2 \psi$$

- **Solve in k-space**

$$\phi_k = \frac{-i\omega + D_a k_\perp^2 + \tau \mu_a \rho^2 k_\perp^4}{-i\omega_e + (D_a - i\omega_i \rho^2) k_\perp^2 + (1+\tau)\mu_a \rho^2 k_\perp^4} h_k$$

- **Radial structure determined by**

$$\frac{dn_e}{dt} = D_a \nabla_\perp^2 n_e + \nabla \cdot J_\parallel / e$$

$$\frac{d\psi}{dt} = \frac{\nabla_\parallel P_e}{e n_e} + \eta J$$

$$\frac{d}{dk_x} \frac{k_\perp^2}{-i\omega_e + \eta k_\perp^2} \frac{d}{dk_x} h = \frac{-\omega\omega_i - i\omega_i (D_a + \mu_a) k_\perp^2 + D_a \mu_a k_\perp^4}{-i\omega_e + (D_a - i\omega_i \rho^2) k_\perp^2 + (1+\tau)\mu_a \rho^2 k_\perp^4} h$$

Drift waves are radiated when the rotation frequency lies in the drift band: $\omega_* > \omega > 0$ so that $0 > \omega_e > -\omega_*$

- **Convective flux**

$$\Gamma_{ExB} = -Nk_y\rho V_{th}\left(1-\frac{\omega}{\omega_*}\right)^2\left|\frac{wh_k}{L_n}\right|^2\left|\frac{\phi_k}{h_k}\right|\sin\delta_k$$

$$\left|\frac{\phi_k}{h_k}\right|^2 = \frac{\omega^2+\left(D_a k_\perp^2+\tau\mu_a\rho^2k_\perp^4\right)^2}{\left(\omega_e+\omega_i\rho^2k_\perp^2\right)^2+\left(D_a k_\perp^2+(1+\tau)\mu_a\rho^2k_\perp^4\right)^2}$$

$$\delta_k = \arctan\frac{D_a k_\perp^2+\tau\mu_a\rho^2k_\perp^4}{\omega} - \arctan\frac{D_a k_\perp^2+(1+\tau)\mu_a\rho^2k_\perp^4}{\omega_e+\omega_i\rho^2k_\perp^2}$$

- **Solution becomes delocalized in drift band**

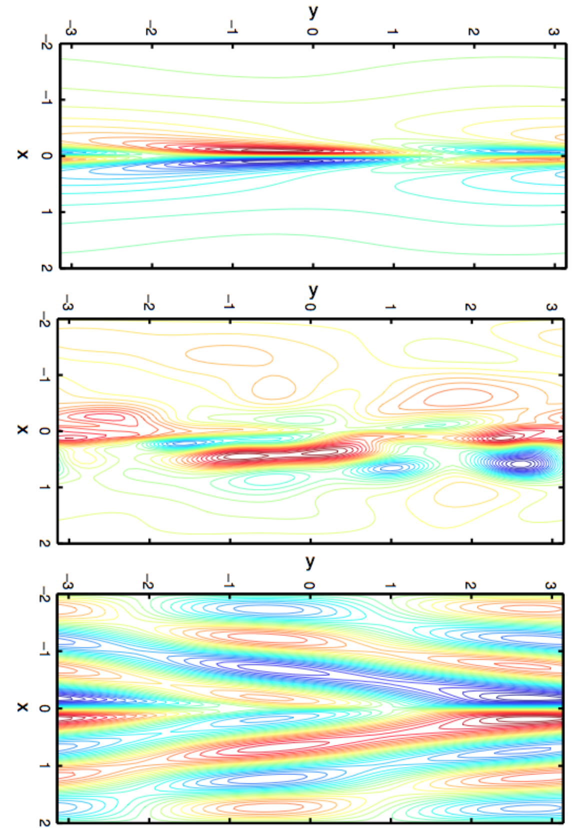

Fig. 7 from
F. Mililtello and F. L. Waelbroeck,
Nucl. Fusion **49** (2009) 065018

Damping of shear flows by additional viscous forces could amplify turbulence saturation amplitude & transport

- Collisional DW dispersion
  - Drift waves damped by diffusion & perp viscosity
  - Convective cells damped by parallel viscosity

$$\omega_e + \omega_e k_\perp^2 \rho^2 = -i\left[Dk_\perp^2 + k_\perp^2\rho^2\left(\nu_\perp + \mu_\perp k_\perp^2\right)\right] + \frac{k_\parallel^2 c_s^2}{\omega + i\left(\nu_\parallel + \mu_\parallel k_\perp^2\right)}$$

$$\omega_{dw} = \frac{\omega_* - i\left[Dk_\perp^2 + k_\perp^2\rho^2\left(\nu_\perp + \mu_\perp k_\perp^2\right)\right]}{\left(1 + k_\perp^2\rho^2\right)} + \ldots$$

$$\omega_{cc} = -i\left(\nu_\parallel + \mu_\parallel k_\perp^2\right) + \ldots$$

- Smaller shear flows are less able to regulate turbulence[1]
  - Flow shearing rate $\omega_{shear} = \mathrm{d}(E_r/B)/\mathrm{d}r$
  - h = 2 or 2/3 (laminar flow)

$$D_{anom} = \frac{\ell_c^2/\tau_c}{1 + \alpha\left(\tau_c \omega_{Shear}\right)^h}$$

- Predator prey model[1] of zonal flow-drift wave interaction predicts that turbulent flux is proportional to zonal flow damping rate

$$\partial_t \phi = +\gamma_\phi \phi - \nu'_\phi \phi^2 - \alpha\phi V^2$$

$$\partial_t V = -\nu_V V + \alpha\phi^2 V$$

$$\partial_t \tfrac{1}{2}\left(\phi^2 + V^2\right) = \gamma_\phi \phi^2 - \nu'_\phi \phi^3 - \nu_V V^2$$

$$\begin{array}{lll} (1) & V = 0 & \phi = \gamma_\phi / \nu'_\phi \\ (2) & V^2 \approx \gamma_\phi / \alpha & \phi^2 \approx \nu_V / \alpha \end{array}$$

Conclusion: Convective transport is the key!

- **It is imperative to understand the transport mechanisms responsible for ELM control and how they scale to future devices**

- **Stochastic transport hypothesis can only be possible in the limit of strong shielding of magnetic perturbations**
  - RMP-induced transport is **convective** not **conductive**
  - Strike-points show splitting in **particle flux**, but not in **heat flux**

- **Investigated 3-field model of shielding & quasilinear transport**
  - FLR effects & anomalous transport should play important roles in the pedestal
  - A single island may exist near the electron resonance where $V_e = 0$
  - Where ions and electrons rotate in opposite directions relative to the perturbation $V_i > 0$ and $V_e > 0$, there can be
    - **Outward magnetic flutter flux**
    - **Radiation of drift waves by small-scale islands**

Additional Material …

Toroidal variations of divertor plasma can be used to mitigate target exhaust

- Non-axisymmetric variations in the electrostatic potential drive both ExB convection and parallel current $J_{||}$
- SOL convection[1] can be used to spread particle and heat fluxes in the divertor
- SOL current[2] can be used to generate magnetic perturbations inside the separatrix that controls pedestal transport & stabillity
- Can be driven either by direct electrical biasing or by passive generation of toroidal divertor asymmetries

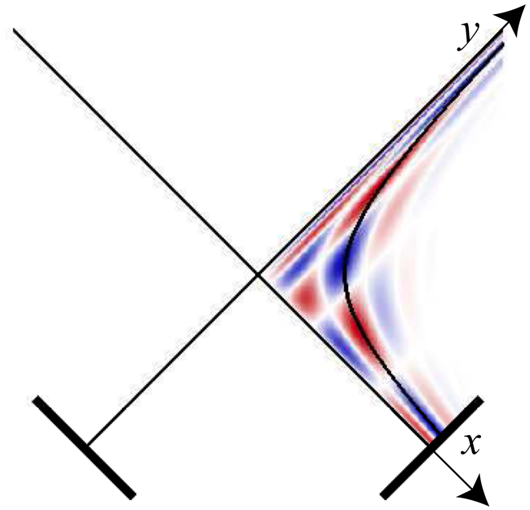

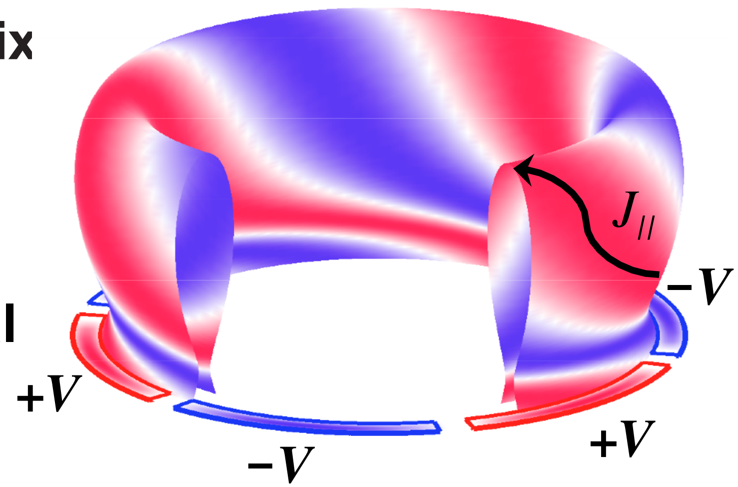

[1]R. H. Cohen and D. D. Ryutov, Nucl. Fusion **37** 621 (1997)
[2]I. Joseph, R. H. Cohen and D. D. Ryutov, Phys. Plasmas **16** 052510 (2009)

Particle & thermal diffusivities can be estimated from power balance in the edge plasma

- Calculated assuming no sources or sinks in the edge plasma

$$\Gamma_N = -D\frac{dn}{dr}$$

$$\Gamma_{E,s} = -\tfrac{3}{2}\chi\frac{dT_s}{dr}$$

- Assume equal power injected into electron and ion channels input power 80 keV NBI
  - $S_N = 1.2\text{x}10^{21}\text{s}^{-1}$
  - $P_{inj} = 9.7$ MW, $P_{oh} = 0.2$ MW
  - $P_{rad,core} = 0.8$ MW
  - $P_e = P_i = 4.5$ MW

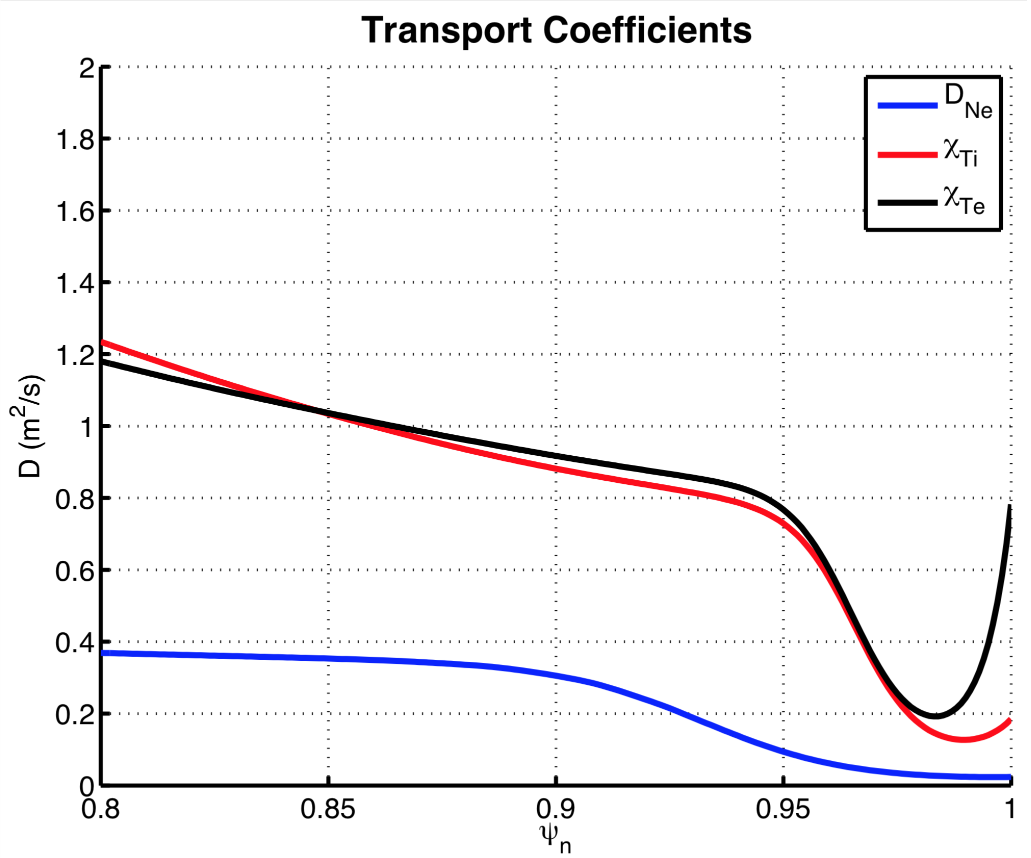

- At such low density, the neutral CX source may be significant in the outer region, as seen in the extremely low value of *D* for $\psi > 95\%$

TRIP3D superimposes external coil fields (Biot-Savart) with Grad-Shafranov axisymmetric equilibrium (EFIT)

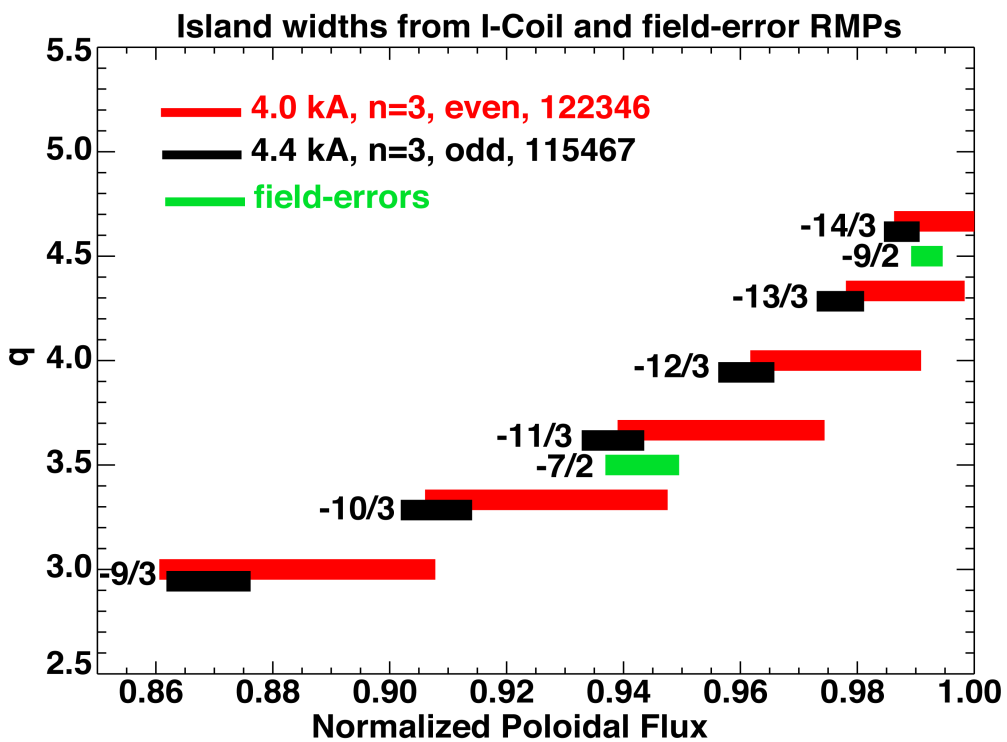

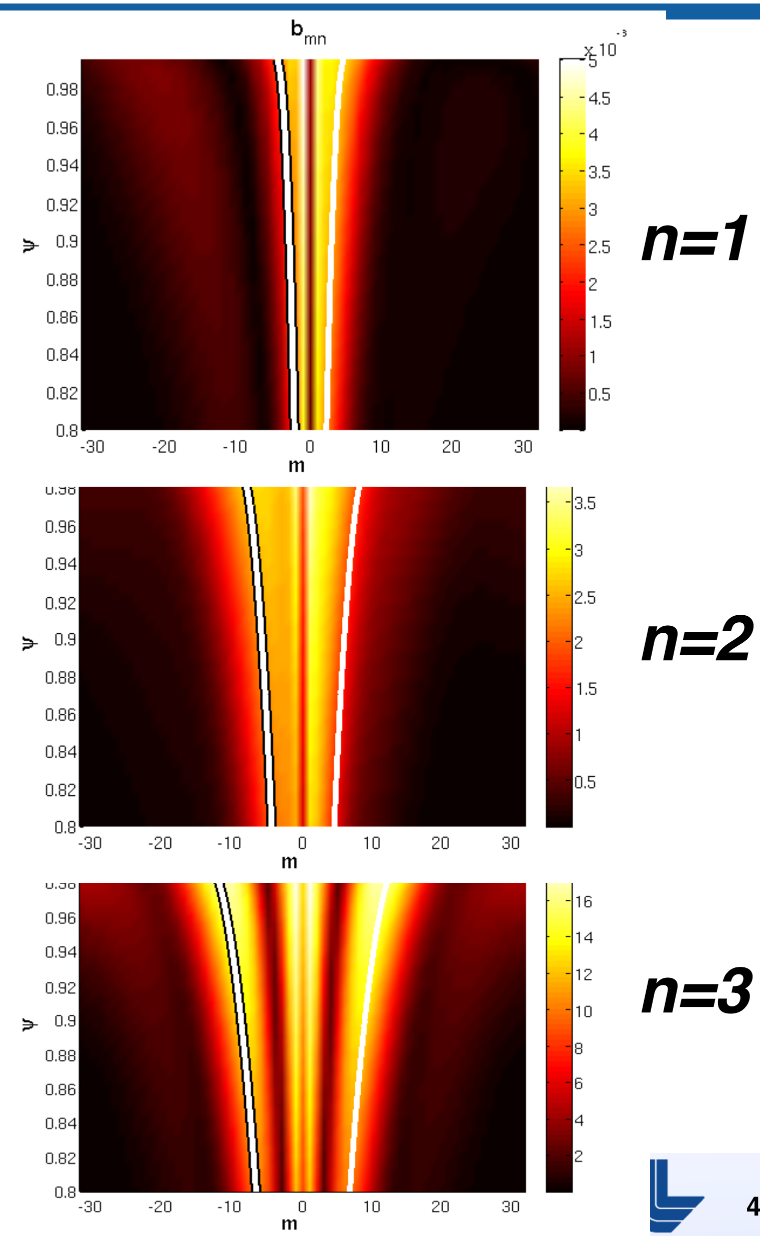

- Island sizes determined from the **vacuum approximation** are large enough to overlap

- Island widths are determined by the resonant $k_{||}=0$ harmonics $\delta B(m=qn)$

Can stochastic field line transport explain the reduction in edge pressure gradient?

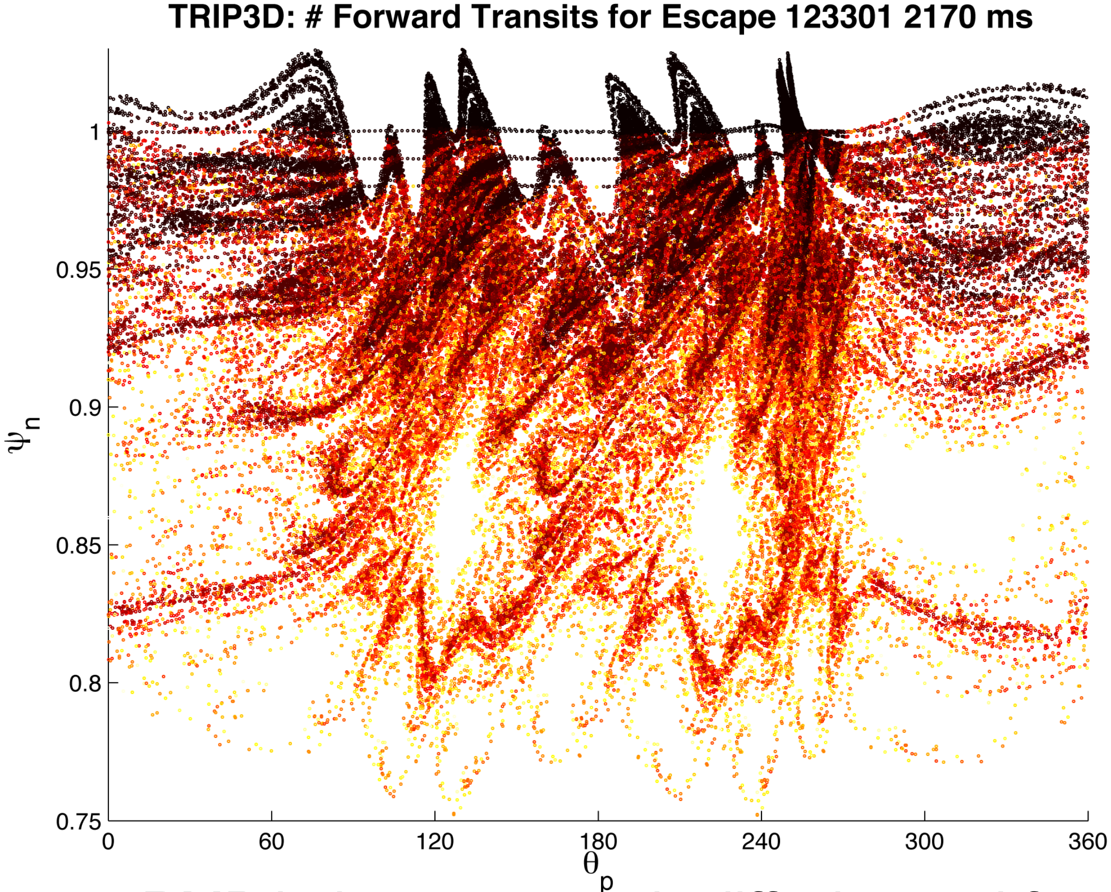

 # toroidal transits for escape

yellow <200

red < 100

black<10

- RMP induces magnetic diffusion and fractal structure in the edge stochastic layer
- TRIP3D B-field model superimposes external RMP-coil fields & EFIT Grad-Shafranov equilibrium

Stochastic transport can be described by considering the quasilinear effect on particle trajectories

- Drift kinetic equation $$\partial_t f + v_{\parallel} \cdot \nabla f + \frac{Ze}{m} E_{\parallel} \cdot \nabla_v f = 0$$

- The initial equilibrium f_0 is close to a Maxwellian, and is constant on the original flux surfaces to lowest order in the gyroradius expansion ρ/L

- A small perturbation δB generates a linear change to the distribution function
$$v_{\parallel} \cdot \nabla_0 f_1 = -v_{\parallel} \frac{\delta B}{B} \cdot \left(\nabla f_0 + \frac{ZeE}{T} f_0 \right) \qquad f_1 = -\frac{|v_{\parallel}|}{v_{\parallel}} \int \frac{\delta B}{B} \left(\nabla f_0 + \frac{ZeE}{T} f_0 \right) d\ell$$

- The perturbed distribution function generates 2nd order fluxes
$$\left. \frac{df_2}{dt} \right|_0 = -\nabla_x \cdot \frac{\delta B}{B} v_{\parallel} f_1 - \nabla_{v_{\parallel}} \frac{\delta B}{B} \cdot \frac{ZeE}{T} f_1 = \left(\nabla_x + \nabla_{v_{\parallel}} \frac{ZeE}{T v_{\parallel}} \right) \Gamma_{fl}$$
$$\Gamma_{fl} = |v_{\parallel}| d_{fl} \left(\nabla f_0 + \frac{ZeE}{T} f_0 \right)$$

- We can identify the magnetic diffusion coefficient as the correlation function
$$d_{\mathrm{fl}} = \int \frac{\delta B}{B}(\ell) \frac{\delta B}{B}(\ell') d\ell' = L_c \left\langle \frac{\delta B}{B}(\ell) \frac{\delta B}{B}(\ell') \right\rangle$$

- The magnetic diffusion coefficient can be estimated via[1] $$d_{\mathrm{fl}} \approx \pi q R \sum_n \left(\frac{\delta B}{B} \right)^2_{m=qn}$$

[1]M.N. Rosenbluth, et al., Nucl. Fusion **6** 297 (1966)

E3D Braginskii fluid transport code developed for stochastic 3D fields was used to calculate transport[1]

Assumes anomalous ⊥ transport in static background field

- Energy equation: (only energy equations used in this study)

$$\boxed{\tfrac{3}{2}n(\partial_t T + u_{\|}\nabla_{\|}T) = \nabla_{\|}\kappa_{\|}\nabla_{\|}T + \nabla_{\perp}\kappa_{\perp}\nabla_{\perp}T + Q_{ei}}$$

- Parallel momentum

$$mn\left(\partial_t u_{\|} + \nabla_{\|}\tfrac{1}{2}u_{\|}^{2}\right) = qnE_{\|} - \nabla_{\|}p - \nabla\cdot\Pi_{\|}$$

- Quasineutral continuity

$$\partial_t n + \nabla_{\|}nu_{\|} = \nabla_{\perp}D_{\perp}\nabla_{\perp}n$$

- Nonlinear sheath BC's (R. Chodura)

$$\boxed{Q = \beta nTC_s\cos\theta_w \sim nT^{3/2}} \qquad \Gamma = nC_s\cos\theta_w \sim nT^{1/2}$$

[1]I. Joseph, et al., Nucl. Fusion **48** 045009 (2008)

E3D uses *Monte-Carlo* fluid elements & field aligned grid to accurately solve highly anisotropic fluid equations

- Heat transport highly anisotropic

$$\kappa_{\parallel} / \kappa_{\perp} = \chi_{\parallel} / \chi_{\perp} \sim 10^{8} - 10^{10}$$

- Stochasticity can generate small scales

$$\ell_{\perp} / \ell_{\parallel} \sim \sqrt{\chi_{\perp} / \chi_{\parallel}} \sim 10^{-4} - 10^{-5}$$

- Fractal connection length structure
- Solution: Monte-Carlo technique
  - Let *T(x,t)* = p.d.f. for heat packets
  - Evolve using Brownian motion

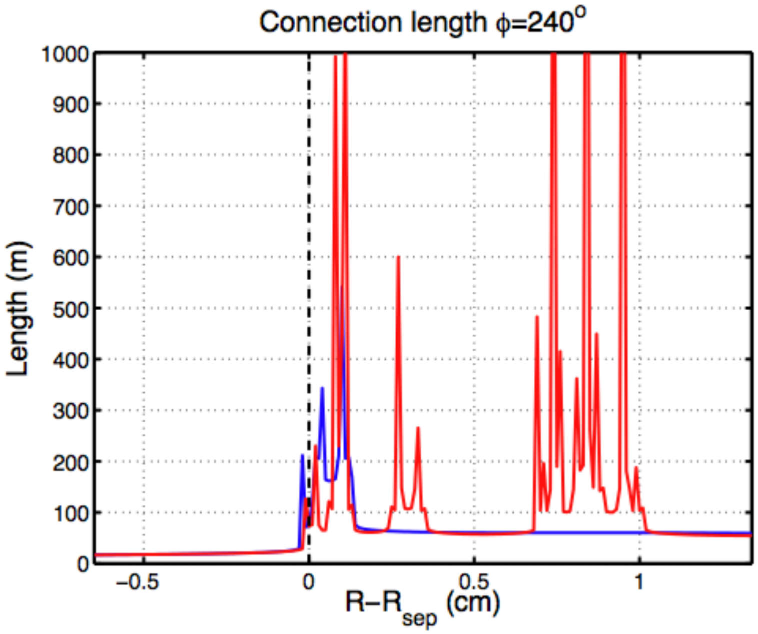

- Use local magnetic coordinate systems to globally cover space
  - Exchange integration for mapping between local subdomains.

E3D simulations[1] determine 3D structure of Te and Ti in the assumed 3D fields

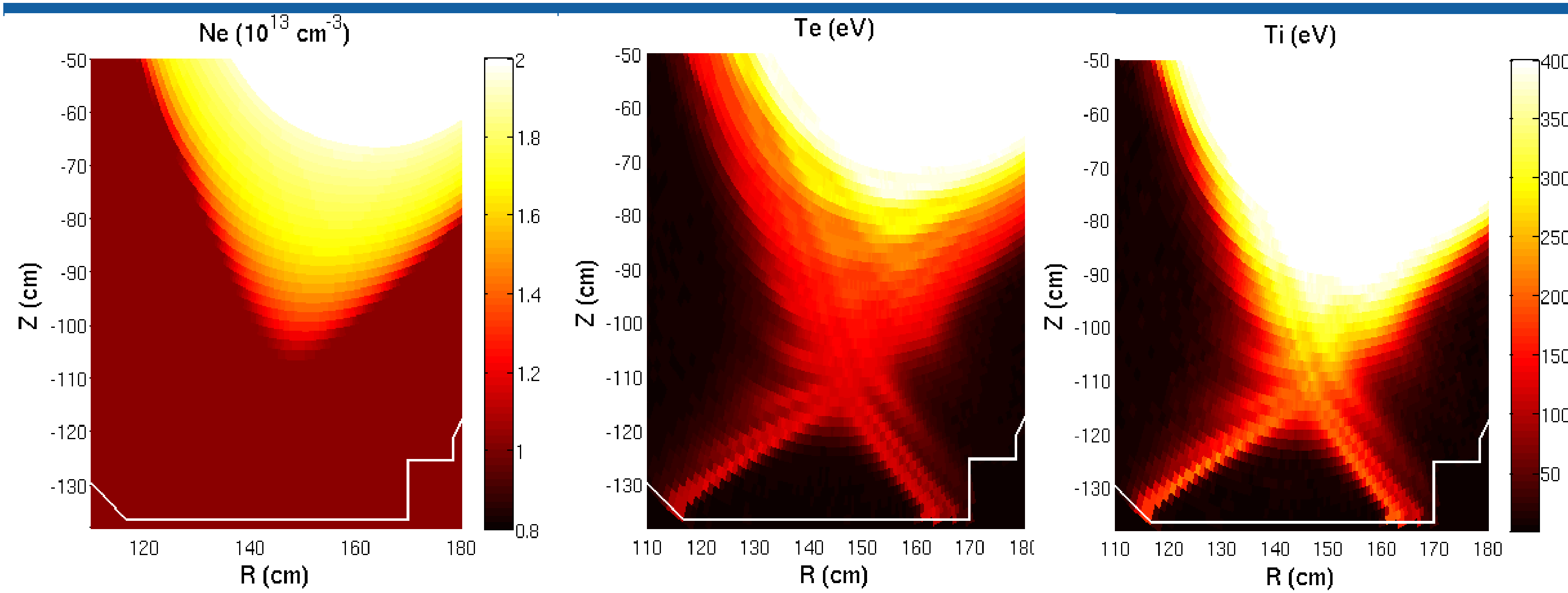

- n_e assumed to be a flux function
- constant D = 1 m^2/s, $\chi_e = \chi_i$ =1.5 m^2/s
- Connection length determines heat flux

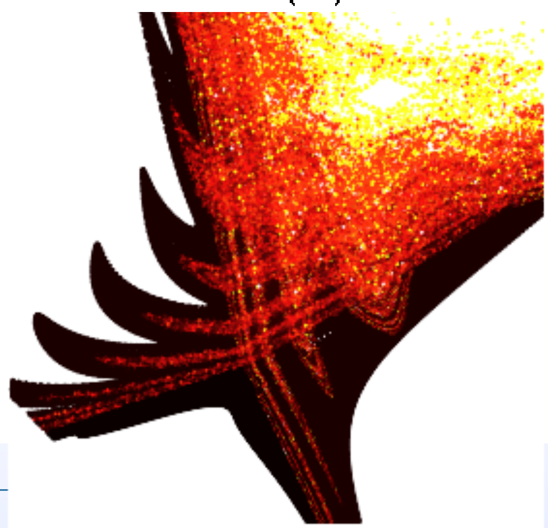

[1] I. Joseph, et al., Nucl. Fusion **48** 045009 (2008)

Inner strike-point heat flux profiles predicted to develop non-axisymmetric structure

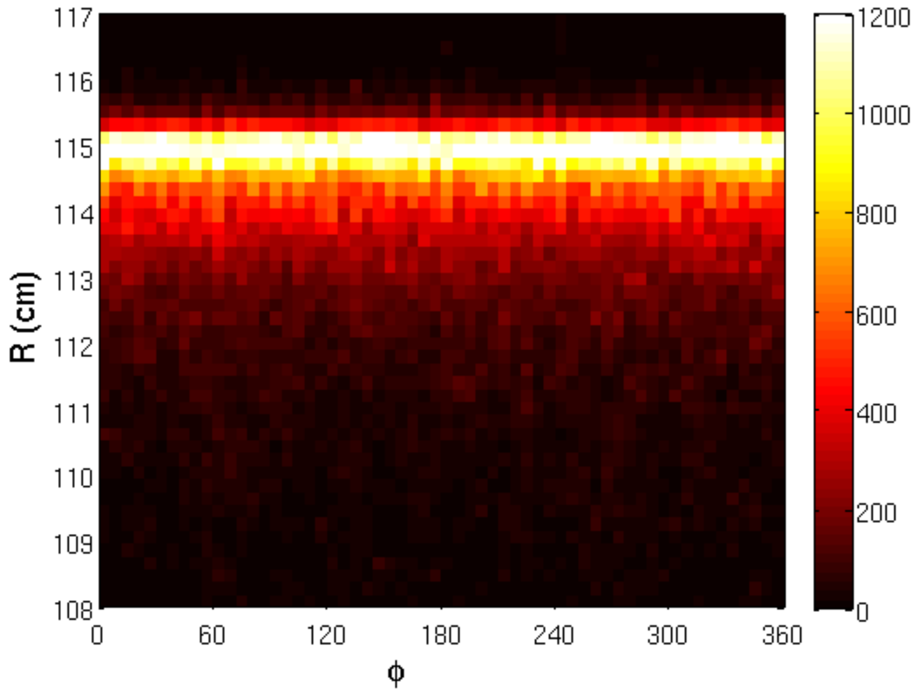

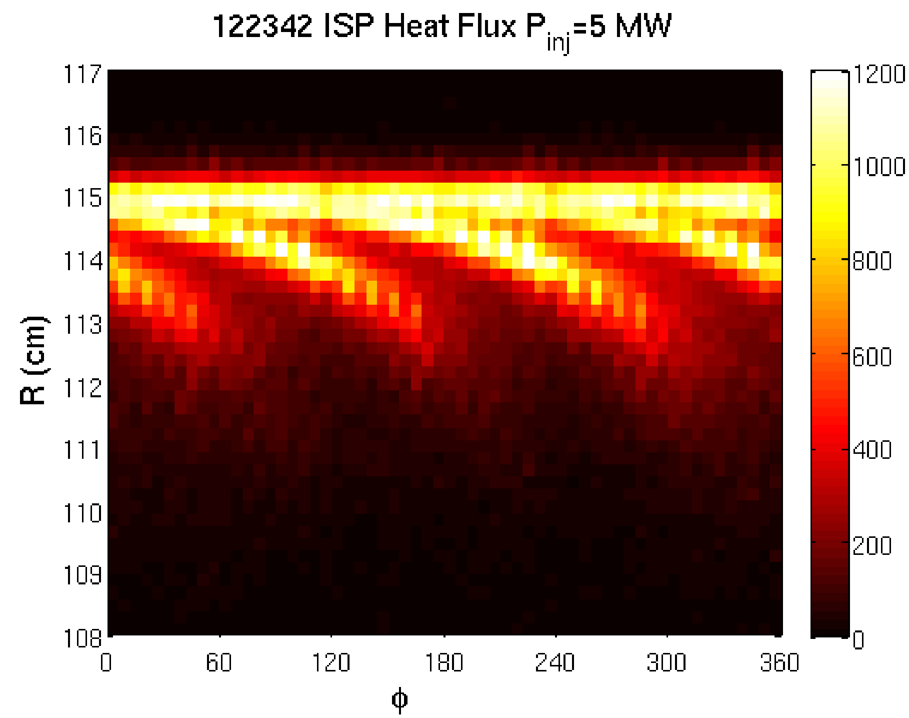

- ***E3D calculations motivated the 2006-2007 experimental campaign***
  - *High resolution Langmuir probe array sweeps to measure fluxes*
  - *New IR camera from TEXTOR at second toroidal location*
  - *Wanted to verify width and phase of structure & variation with edge q_{95}*

Detailed heat flux calculated at fixed toroidal location

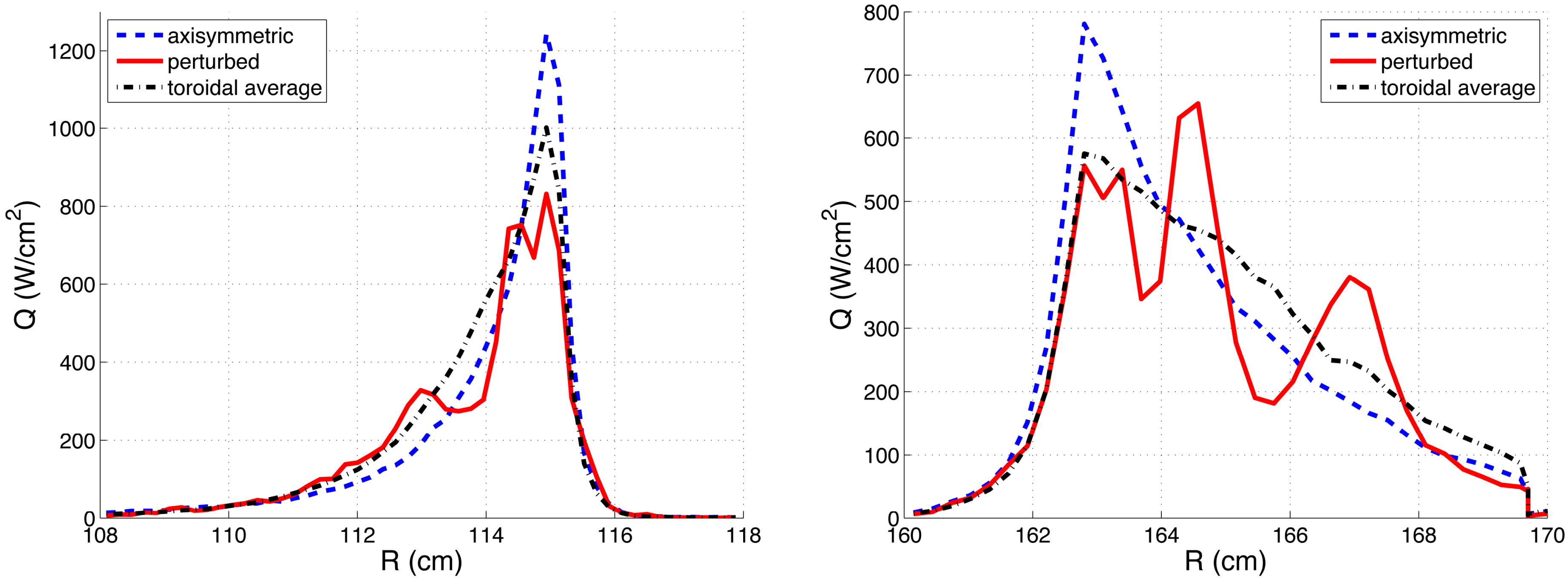

- Field lines efficiently loaded with heat upstream
- Effective area for flux deposition predicted to increase by 50%
  - Direct field line contact area increased, but
  - Perpendicular decay length decreased due to higher temperature
  - Optimization requires accurate calculation of Te and Ti at target
- Rotating tearing activity should produce equivalent toroidally averaged profile

Dramatic heat flux splitting was originally observed in high collisionality perturbation experiments

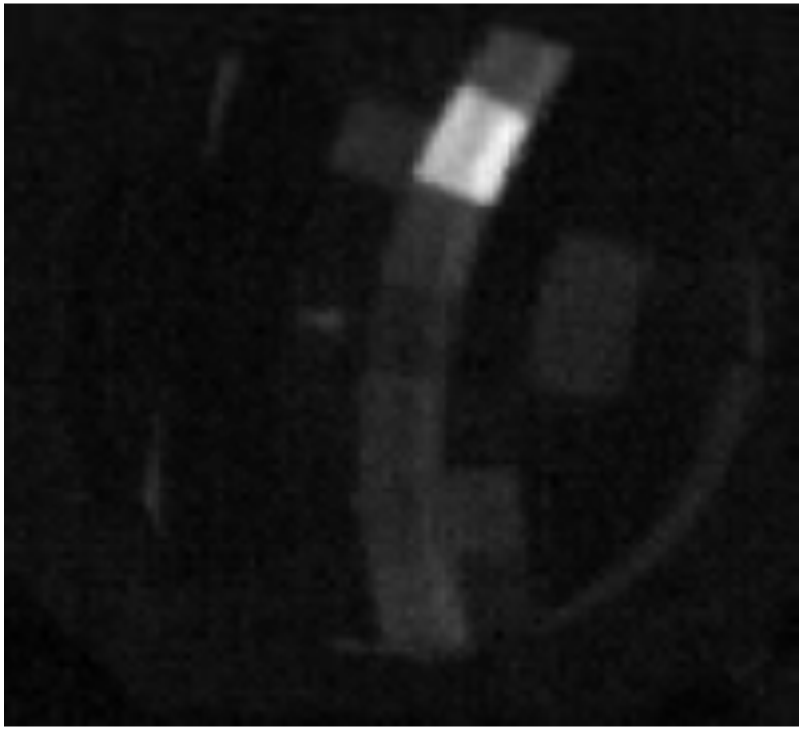

- Relatively weak fields observed to have 3x larger effect
  - N=1 plasma response fields are implicated
- Motivates study of field line structure at divertor target
- Can we use this technique to spread heat flux in reactor designs?

[1] T. E. Evans, et al., J. Nucl. Mater. **363-365** 570 (2007)

Dramatic heat flux splitting was originally observed in high collisionality cases without pumping

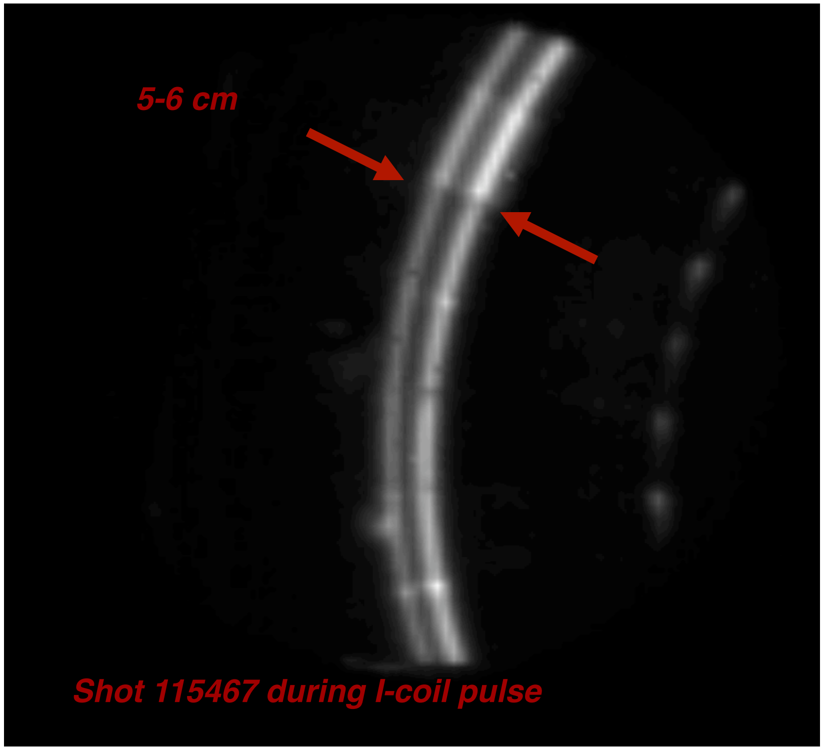

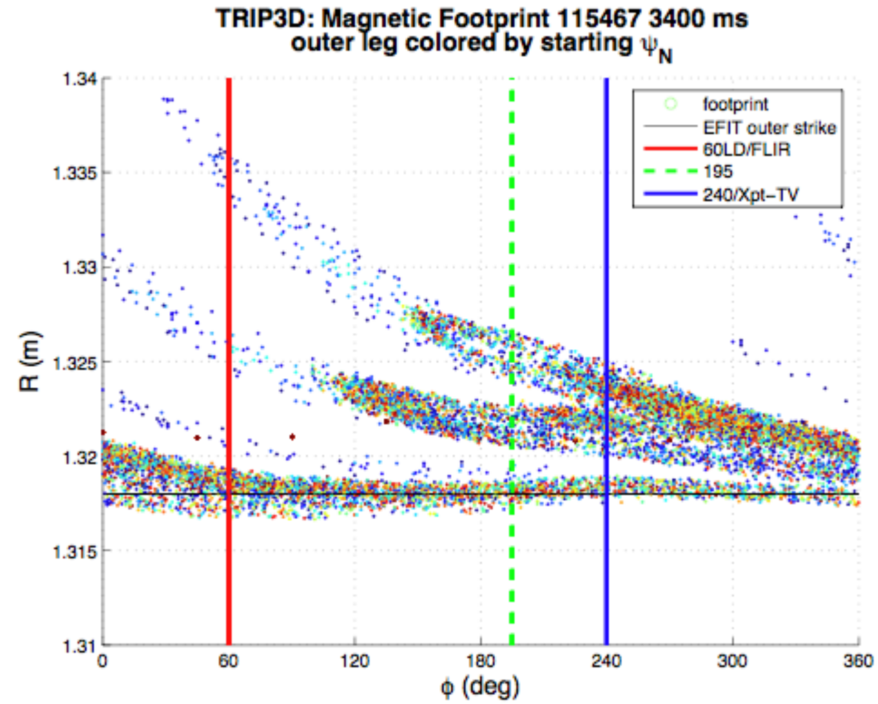

- Odd parity RMP ~5X weaker than even parity
- But appears to have 2 striations, not 3 (maybe more n=1?)
  - 5-6 cm measured width, but only 2 cm predicted?

The outer lobes are thermally isolated from the interior except during radial transport events

- **ISP splitting in IR measurements** **#129194**

ELM & RMP(no ELM suppression) | **ELM supression** | **right after pellet with RMP**

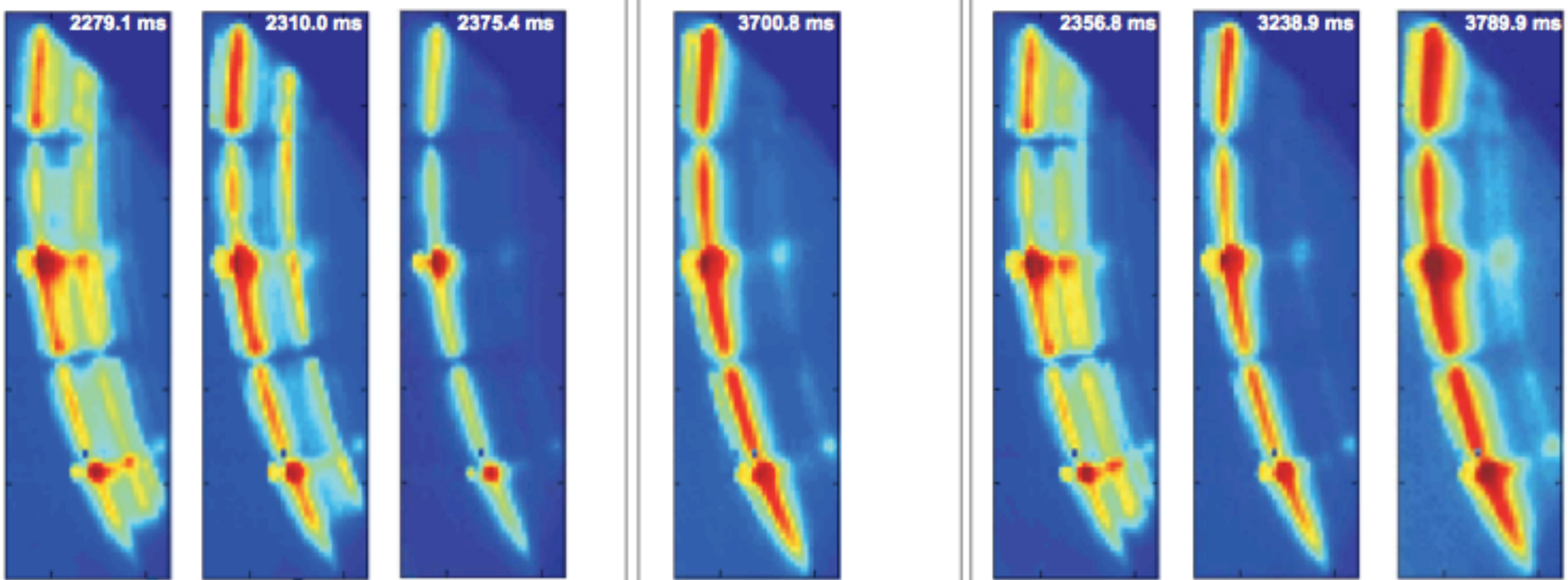

ELM heat expell fills lobes, i.e. fillamentary ELM structure is governed by RMP helicity

very tiny imprint of outer lobe in heat flux

pellet cause sufficient convective heat expell to map magnetic footprint

⇒ **increased radial heat flux is needed to detect SP splitting**

(M Jakubowski & O Schmitz, FZ-Julich)